Metallic Magnetic Calorimeters for Neutrino Physics

Loredana Gastaldo

Kirchhoff Institute for Physics, Heidelberg University

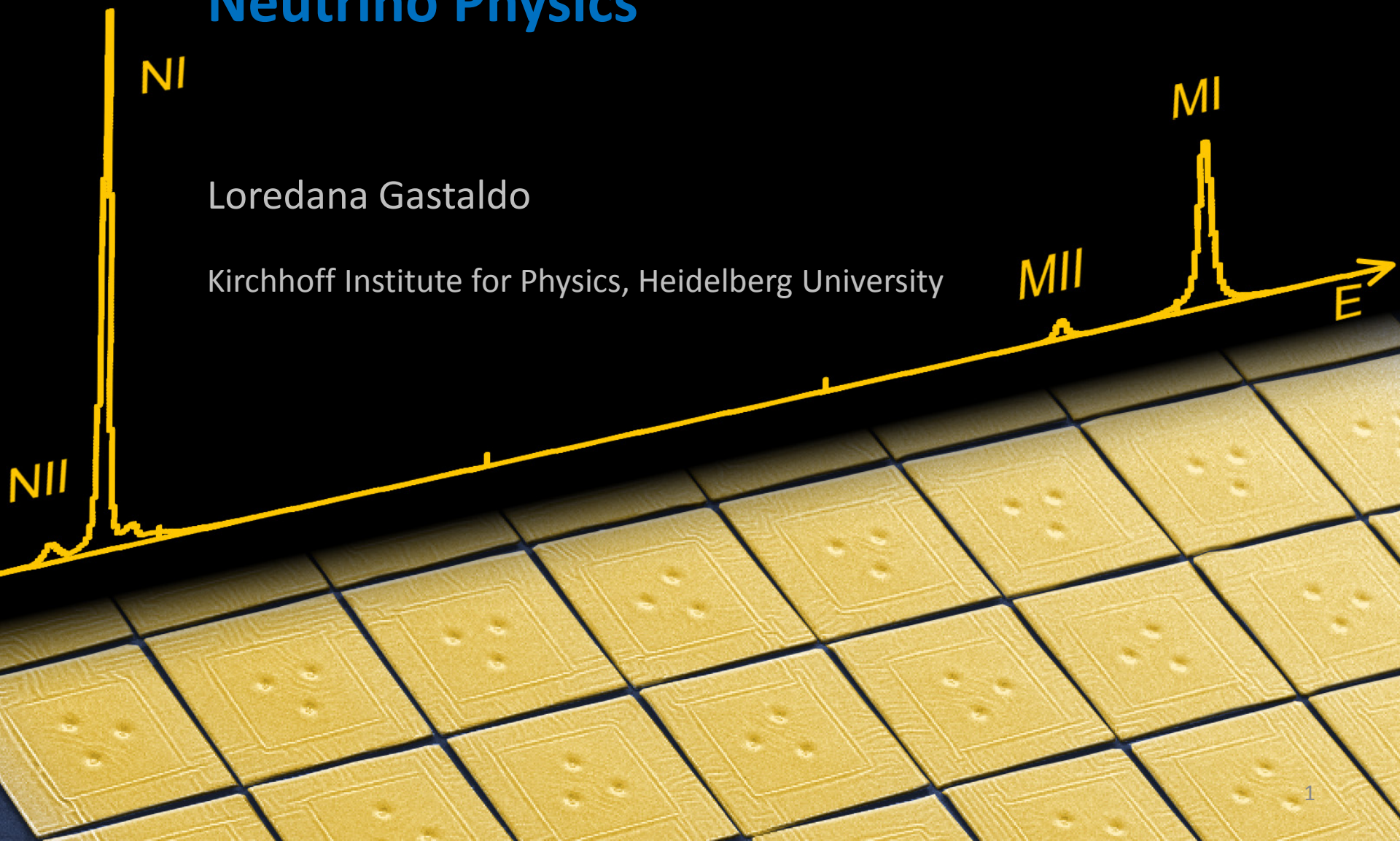

First conference on Low Temperature Detectors

…for Neutrino and Dark Matter

Castle Ringberg, Bavaria, 1987

First conference on Low Temperature Detectors

Program

1.	Update on Neutrinos, Dark Matter, and Cryogenic Detection.	L. Stodolsky
2.	New Results on the Basic Properties of Superheated Granules Detectors.	L. Gonzales-Mestres and D. Perret-Gallix
3.	Investigation of Superconducting Tin Granules for a Low-Energy Neutrino or Dark Matter Detector.	K. Pretzl
4.	SQUID Detection of Superheated Granules.	A. Kotlicki
5.	VLSI Superconducting Particle Detectors.	0. Liengme
6.	"Minicylinder" Design for Solar Neutrino Detection (A naive proposal).	G.Vesztergombi
7.	Electron Beam Detection with Superheated Superconducting Grains.	A. de Bellefon
8.	Monte Carlo Simulation of a 2β-Decay Experiment with Superconducting-Superheated Tin Granules.	A.F. Pacheco
9.	Solar Neutrino Indium Detector Using Superheated Granules.	G. Waysand
10.	An Indium Solar Neutrino Experiment.	N.E. Booth
11.	Cryogenic Detection of Particles, Development Effort in the United States.	B. Sadoulet
12.	Calorimetric Detectors at Low Temperatures.	F.v. Feilitzsch, F. Probst, and W, Seidel
13.	The Possible Impact of Thermal Detectors in Nuclear and Subnuclear Physics.	E. Fiorini
14.	Considerations on Front End Electronics for Bolometric Detectors with Resistive Readout.	D.V. Camin
15.	Coherent Neutrino-Nucleus Elastic Scattering in Ultralow-Temperatures Calorimetric Detectors.	T.O. Niinikoski
16.	Data Acquisition and Analysis of Calorimetric Signals.	A. Rijllart
17.	The Use of Rotons in Liquid Helium to Detect Neutrinos	G.M. Seidel

First conference on Low Temperature Detectors

Program

1.	Update on Neutrinos, Dark Matter, and Cryogenic Detection.	L. Stodolsky
2.	New Results on the Basic Properties of Superheated Granules Detectors.	L. Gonzales-Mestres and D. Perret-Gallix
3.	Investigation of Superconducting Tin Granules for a Low-Energy Neutrino or Dark Matter Detector.	K. Pretzl
4.	SQUID Detection of Superheated Granules.	A. Kotlicki
5.	VLSI Superconducting Particle Detectors.	0. Liengme
6.	"Minicylinder" Design for Solar Neutrino Detection (A naive proposal).	G.Vesztergombi
7.	Electron Beam Detection with Superheated Superconducting Grains.	A. de Bellefon
8.	Monte Carlo Simulation of a 2β-Decay Experiment with Superconducting-Superheated Tin Granules.	A.F. Pacheco
9.	Solar Neutrino Indium Detector Using Superheated Granules.	G. Waysand
10.	An Indium Solar Neutrino Experiment.	N.E. Booth
11.	Cryogenic Detection of Particles, Development Effort in the United States.	B. Sadoulet
12.	Calorimetric Detectors at Low Temperatures.	F.v. Feilitzsch, F. Probst, and W, Seidel
13.	The Possible Impact of Thermal Detectors in Nuclear and Subnuclear Physics.	E. Fiorini
14.	Considerations on Front End Electronics for Bolometric Detectors with Resistive Readout.	D.V. Camin
15.	Coherent Neutrino-Nucleus Elastic Scattering in Ultralow-Temperatures Calorimetric Detectors.	T.O. Niinikoski
16.	Data Acquisition and Analysis of Calorimetric Signals.	A. Rijllart
17.	The Use of Rotons in Liquid Helium to Detect Neutrinos	G.M. Seidel

17th conference on Low Temperature Detectors

Kurume, Japan, 2017

More than 300 participants

Neutrino Physics with LTDs

Experiments for the determination of the electron neutrino effective mass

(+ Searching for evidence of sterile neutrinos)

ECHo

HOLMES

Experiments for the search of neutrinoless double beta decay

CUORE

LUMINEU

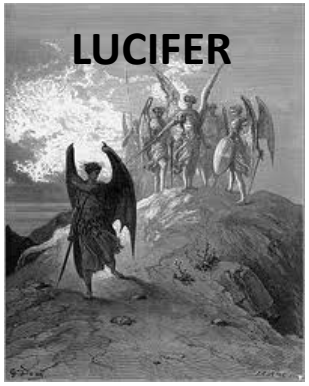

CUPID

AMoRE

Measurements of the coherent electron neutrino nucleus scattering

RICOCHET

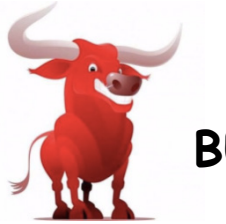

Nν-CLEUS

BULLKID

Detection of the cosmic neutrino background

P on-
T ecorvo
O bservatory for
L ight,
E arly-universe,
M assive-neutrino
Y ield

Neutrino Physics with LTDs

Experiments for the determination of the electron neutrino effective mass

(+ Searching for evidence of sterile neutrinos)

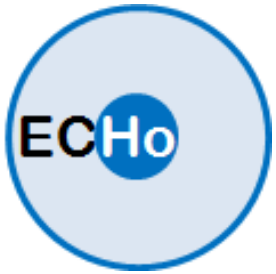

Experiments for the search of neutrinoless double beta decay

AMoRE

Table of contents

Low temperature micro-calorimeters

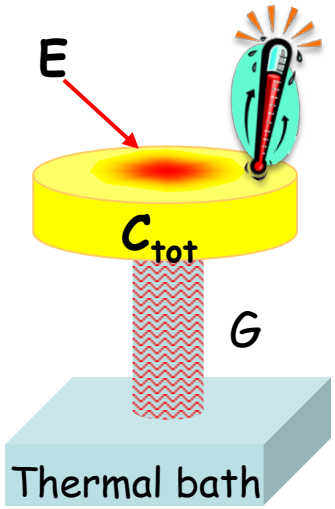

$$\Delta T \cong \frac{E}{C_{\text{tot}}}$$

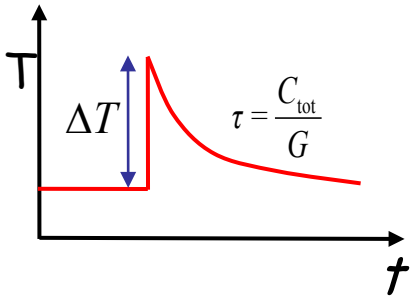

E = 10 keV

C_{tot} = 1 pJ/K

→~ 1 mK

- Very small volume
- Working temperature below 100 mK
  small specific heat
  small thermal noise
- **Very sensitive temperature sensor**

Temperature sensors

Resistance of highly doped semiconductors

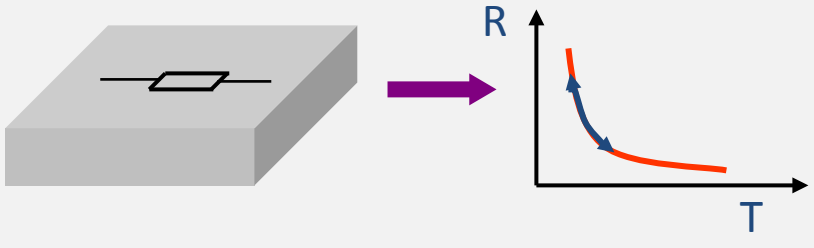

Resistance at superconducting transition,TES

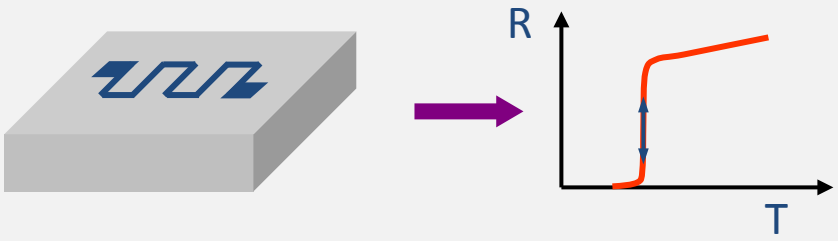

Magnetization of paramagnetic material, MMC

Temperature sensors

Resistance of highly doped semiconductors

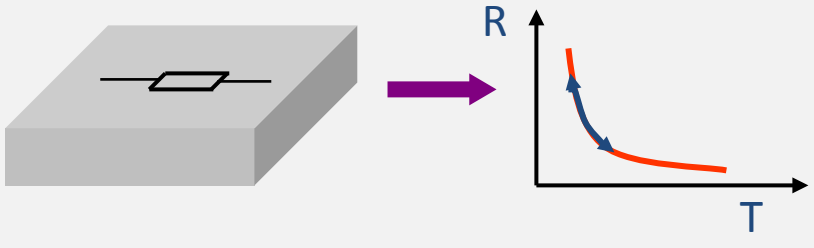

Resistance at superconducting transition,TES

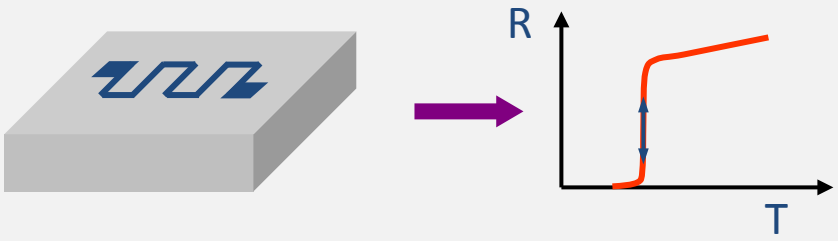

Magnetization of paramagnetic material, MMC

Metallic magnetic calorimeters (MMCs)

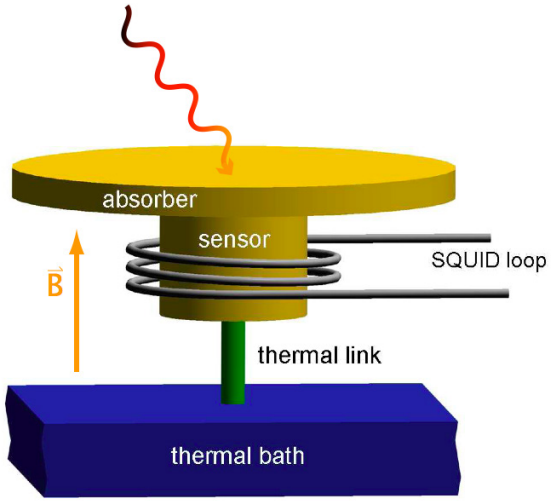

A. Fleischmann et al.,
AIP Conf. Proc. **1185**, 571, (2009)

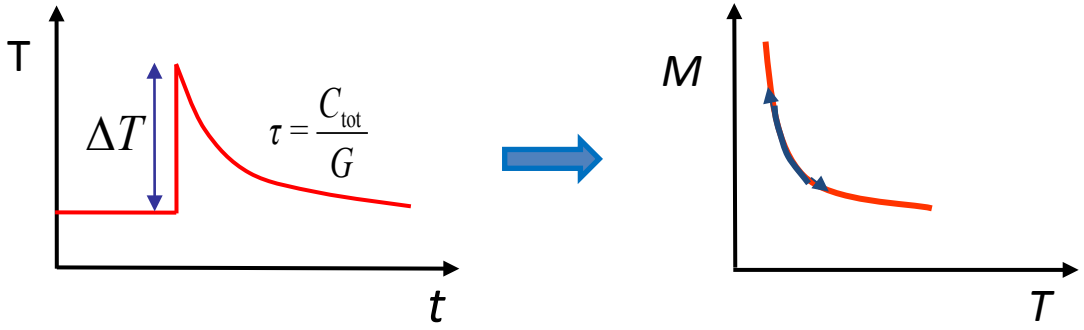

- Paramagnetic Au:Er sensor
  Ag:Er

$$\Delta\Phi_S \propto \frac{\partial M}{\partial T}\Delta T \rightarrow \Delta\Phi_S \propto \frac{\partial M}{\partial T}\frac{E}{C_{sens}+C_{abs}}$$

Metallic magnetic calorimeters (MMCs)

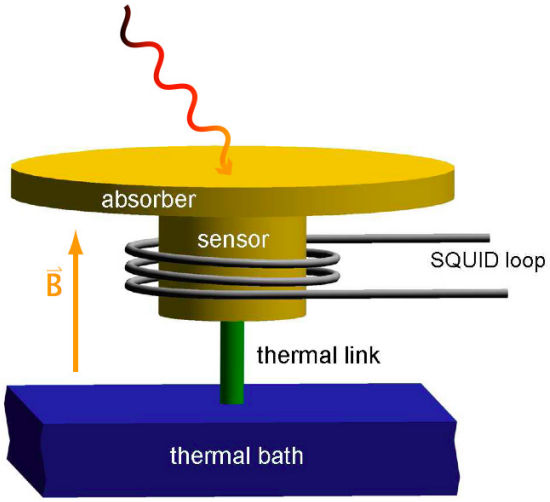

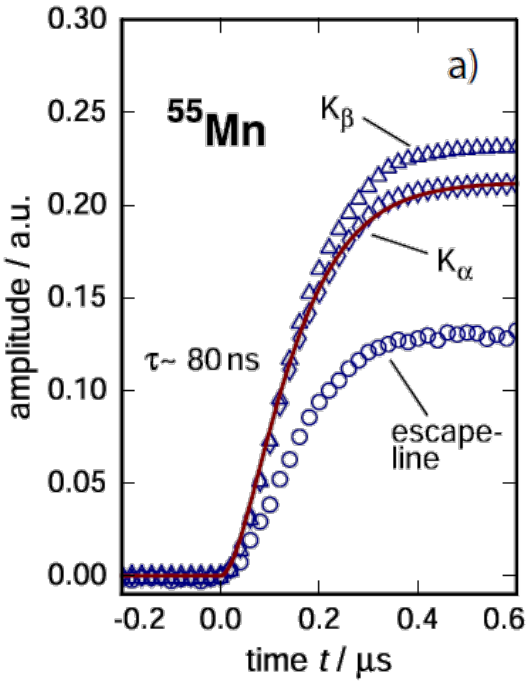

Fast risetime

→ Reduction un-resolved pile-up

Metallic magnetic calorimeters (MMCs)

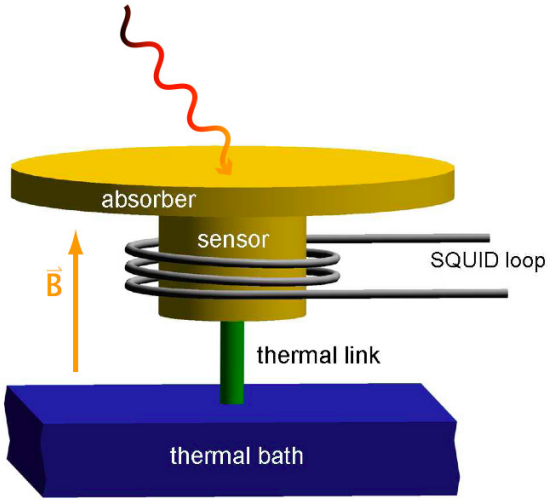

Fast risetime

→ Reduction un-resolved pile-up

Extremely good energy resolution

→Reduced smearing in the end point region

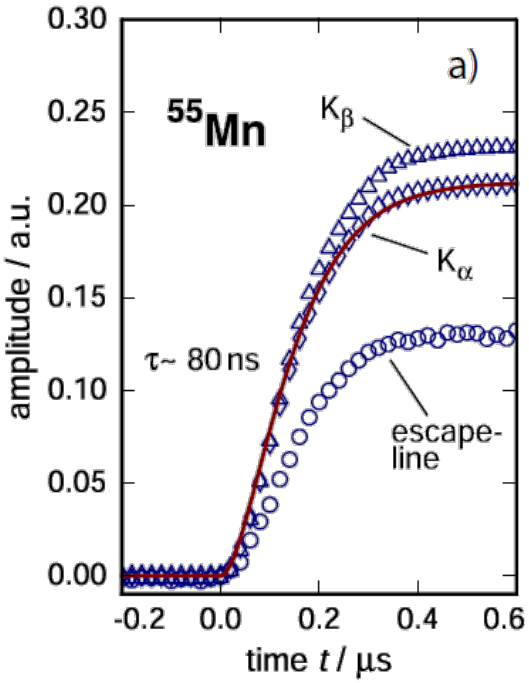

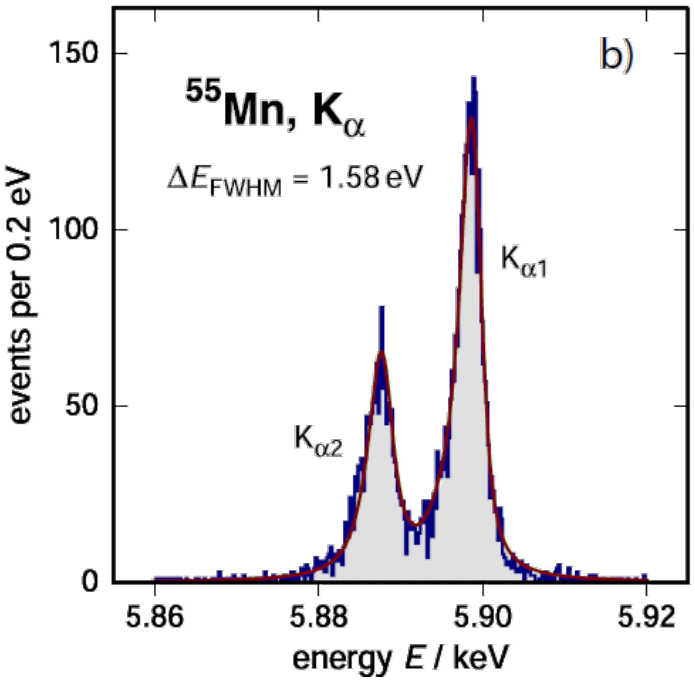

Metallic magnetic calorimeters (MMCs)

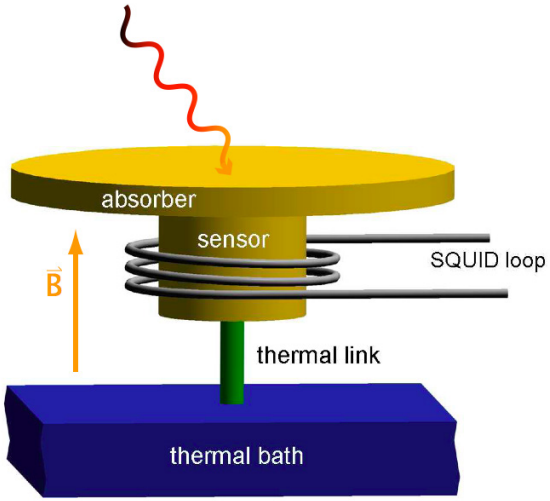

Fast risetime

→ Reduction un-resolved pile-up

Extremely good energy resolution

→Reduced smearing in the end point region

Excellent linearity

→ precise definition of the energy scale

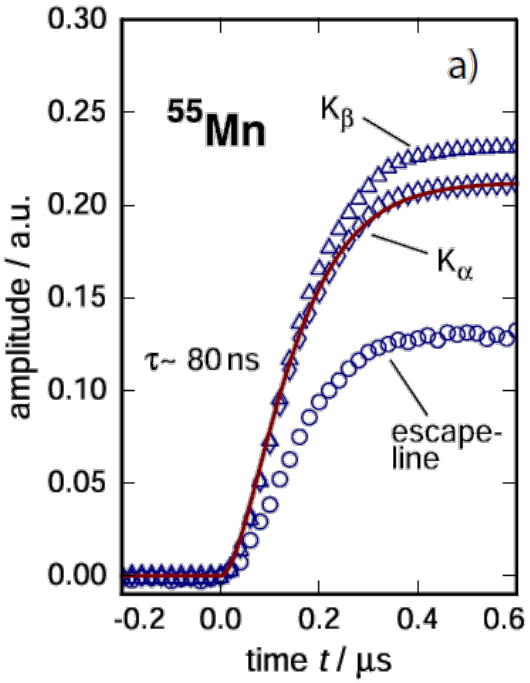

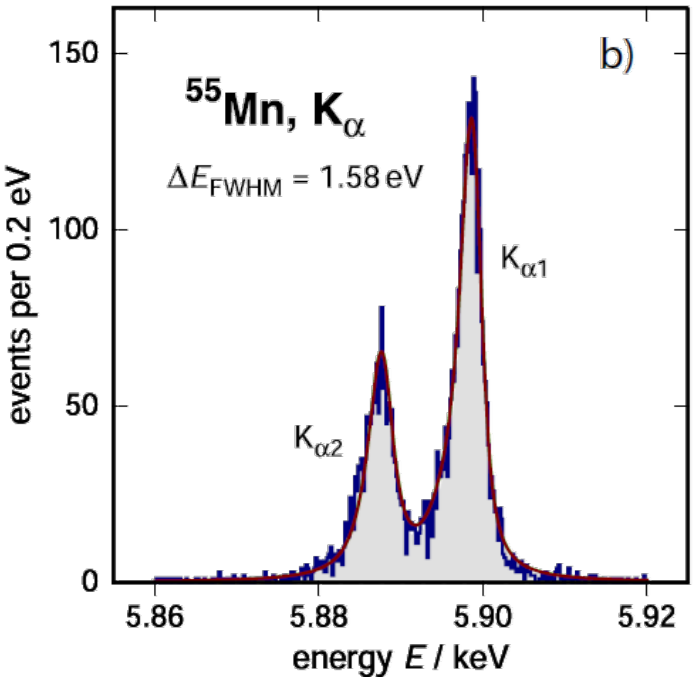

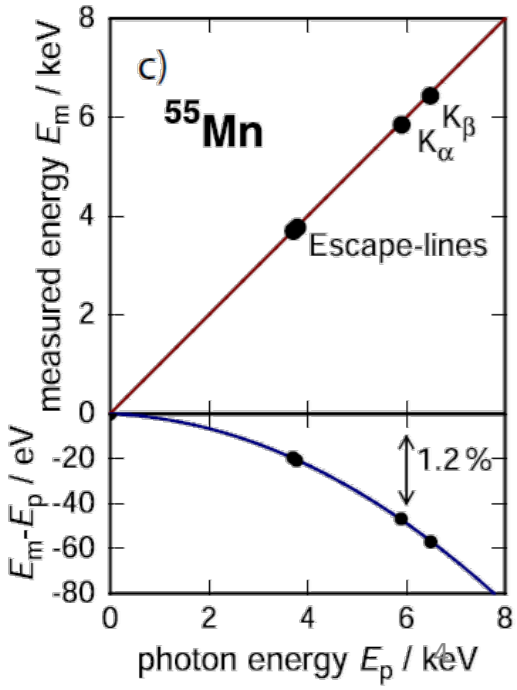

MMCs: Planar Geometries

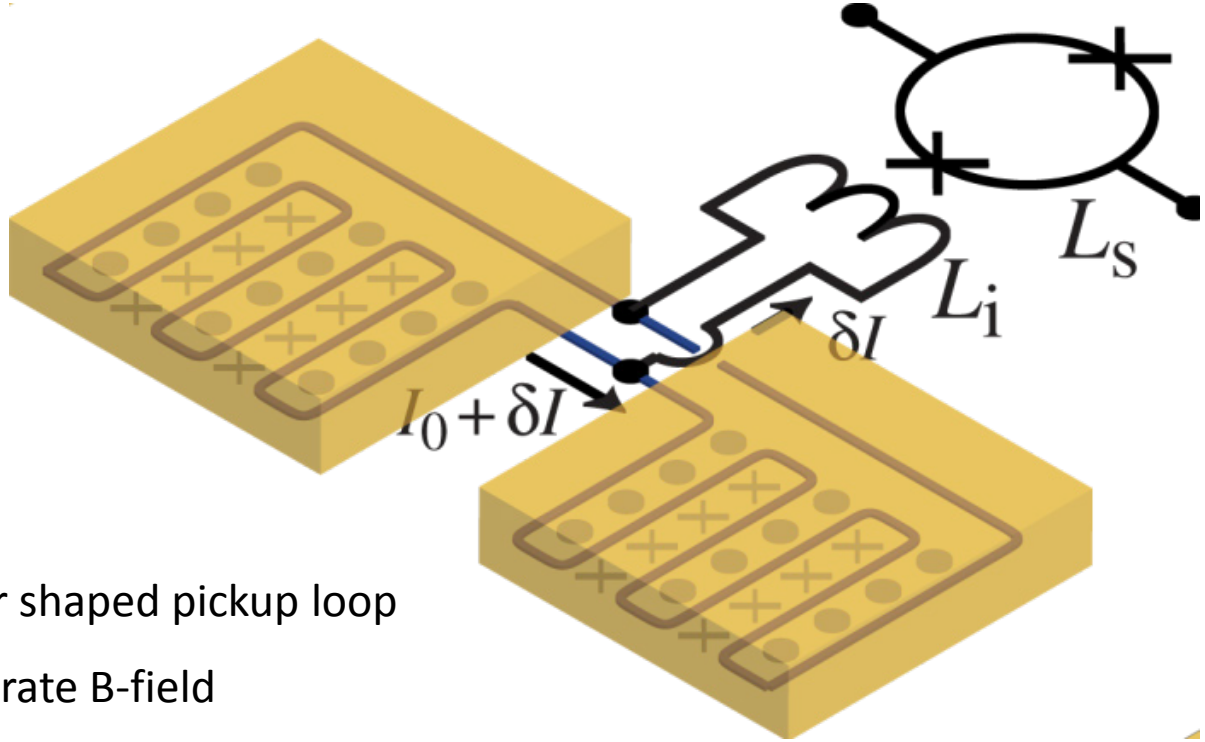

Double meander geometry

- planar *T*-sensor
- superconducting meander shaped pickup loop
- persistent current to generate B-field
- transformer-coupled to SQUID

- the two pixels show signals of opposite polarity
  -> fairly insensitive to chip *T*

maXs - high resolution x-ray spectroscopy

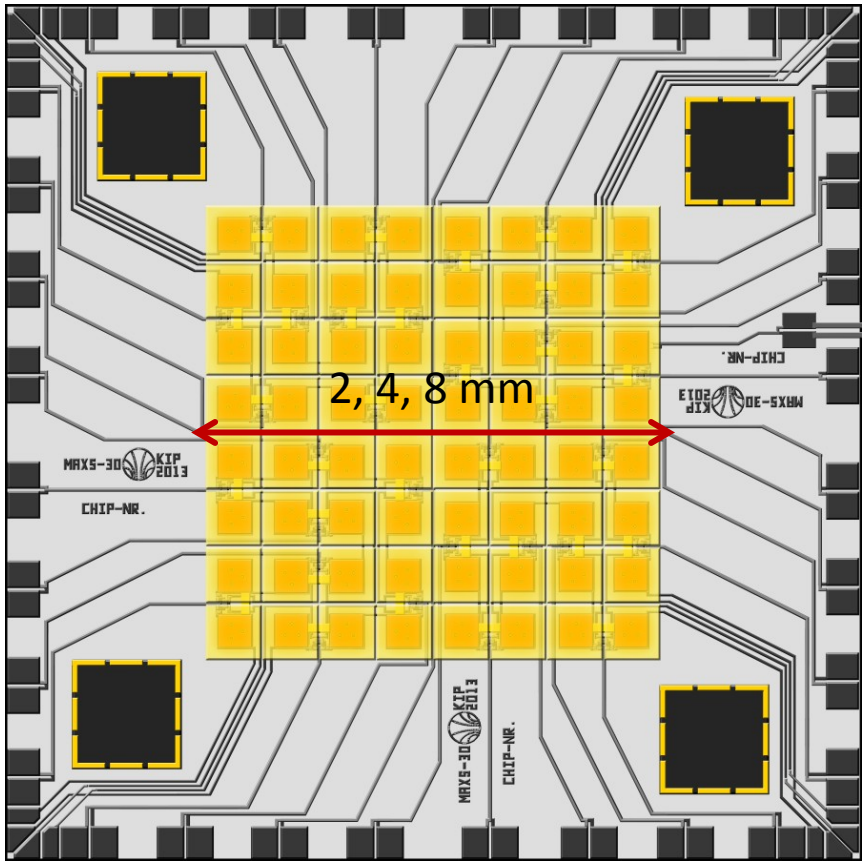

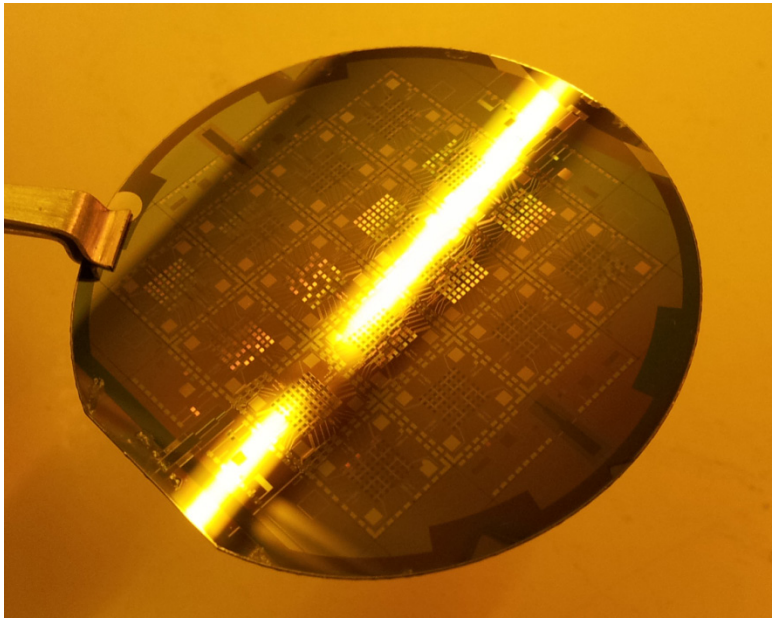

maXs-20/30/200:

- 8×8 pixels for photons up to 20/30/200 keV
- with ΔE_{FWHM} = 2/5/30 eV
- **32 two-stage dc-SQUIDs**

maXs-30: example of assembly

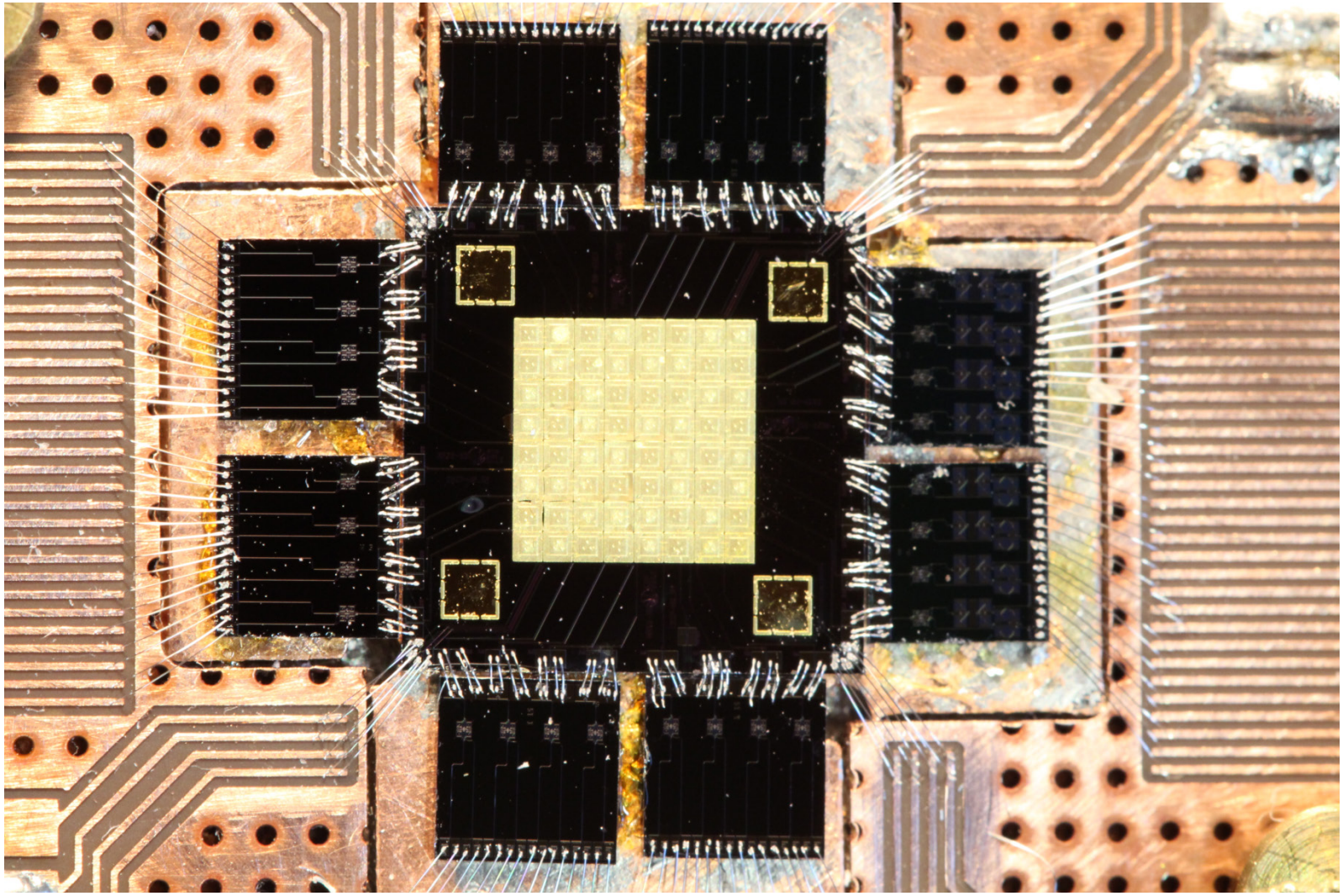

MOCCA a 4k-pixel MMC camera for molecules

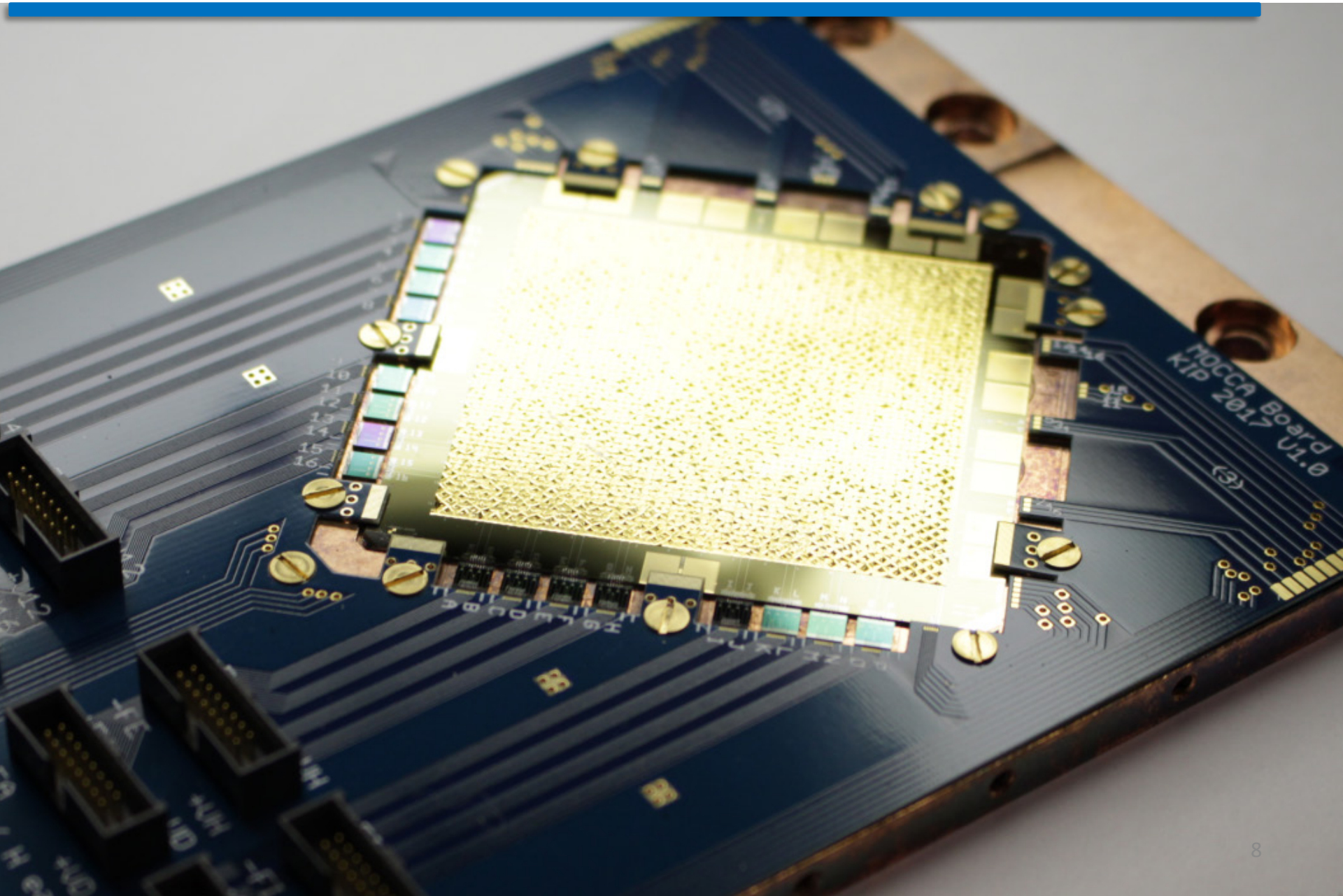

MMCs: Microfabrication

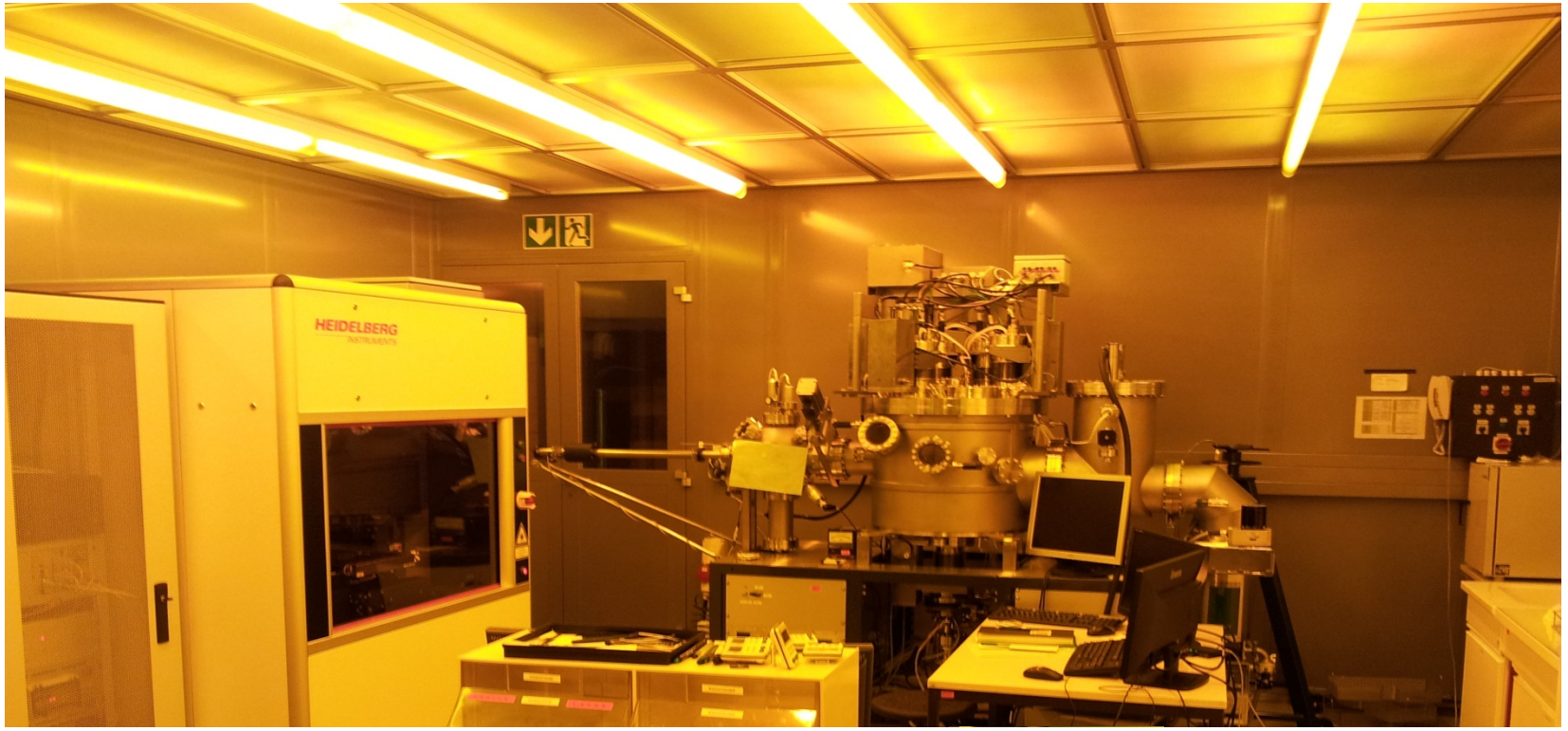

maXs20: 1d-array for soft x-rays

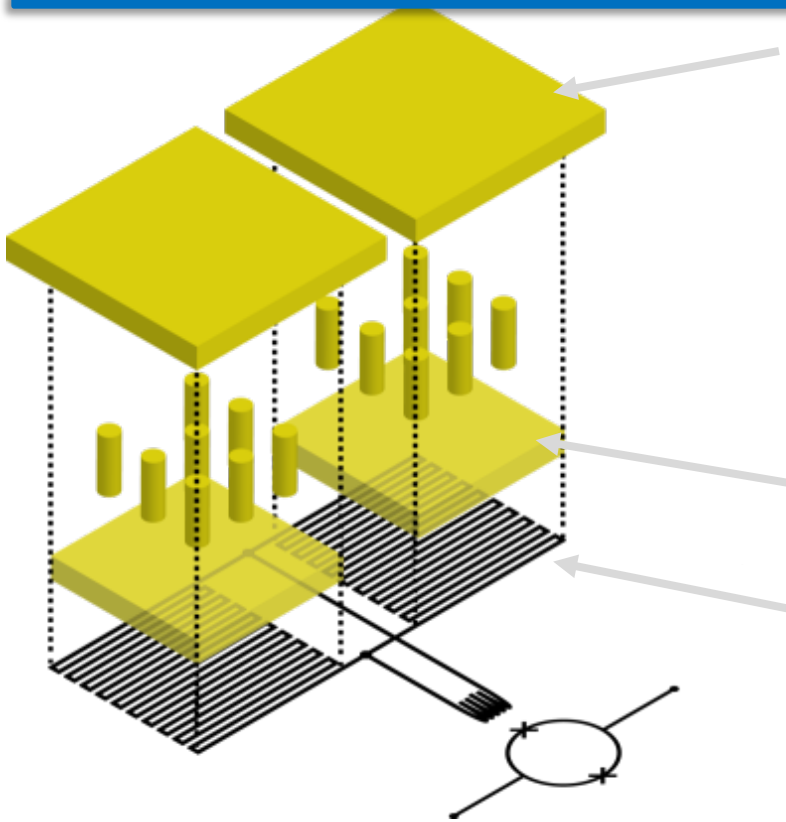

- **1×8 x-ray absorbers**
  - **250μm×250μm** gold**, 5μm thick**
  - **98%** Qu.-Eff. @ 6 keV
  - electroplated into photoresist mold (RRR>15)
  - **mech/therm contact to sensor by stems** to prevent loss of initially hot phonons
- **Au:$^{166}Er_{300ppm}$ temperature sensors**
  - co-sputtered from pure Au and high conc. AuEr target
- **Meander shaped pickup coils**
  - 2.5 μm wide Nb lines
  - **I_c ≈ 100mA**
- **On-chip persistent current switch** (AuPd)

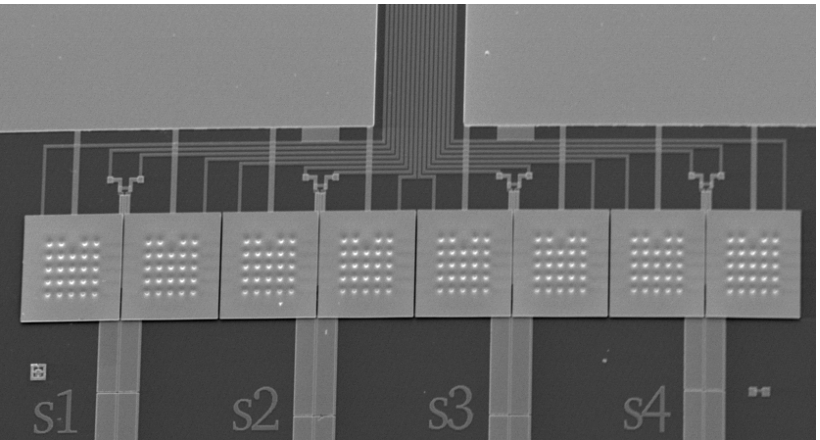

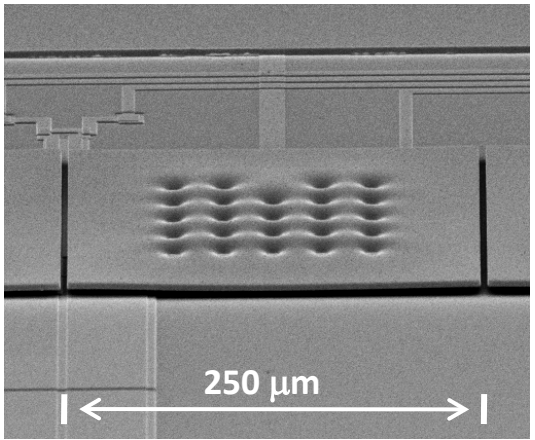

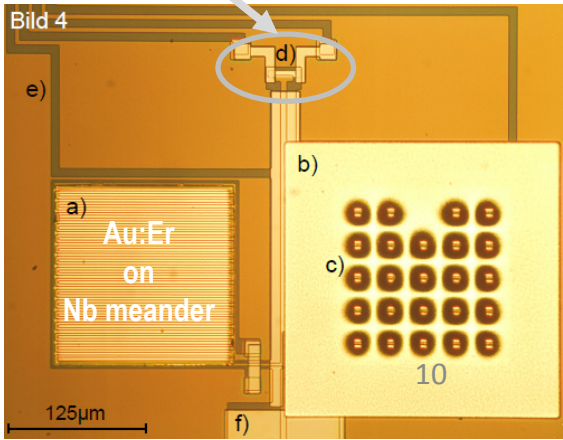

MMC read-out

- Two-stage SQUID read-out

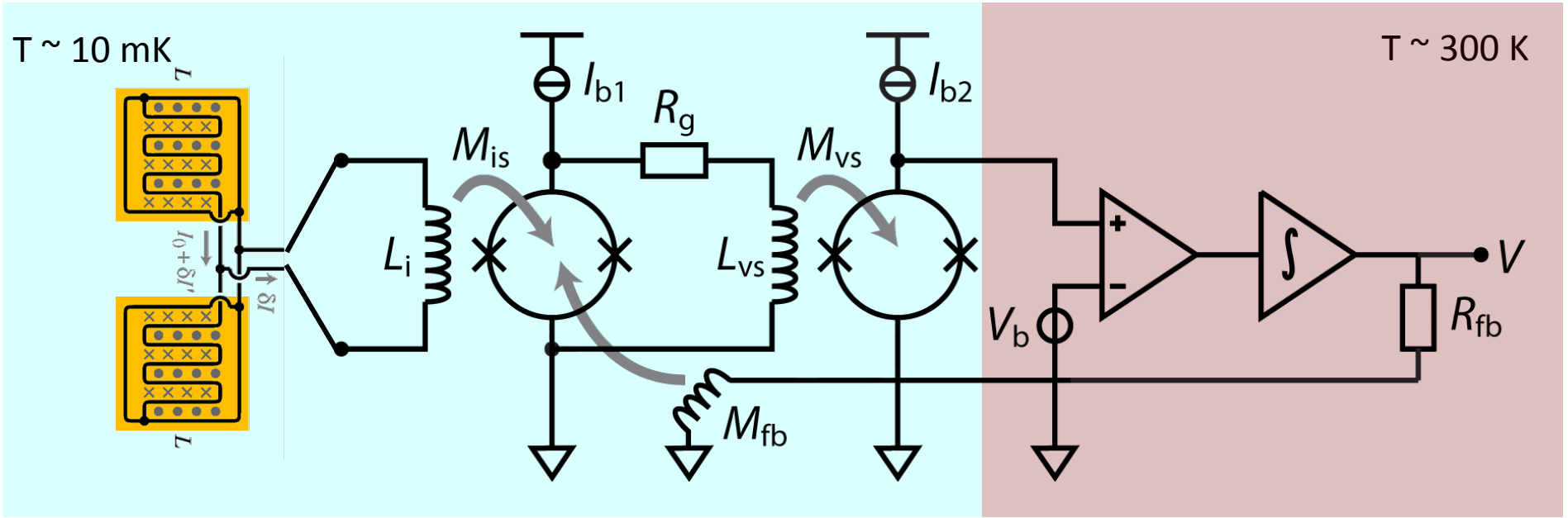

Multiplexing readout

Microwave SQUID multiplexing
Single HEMT amplifier and 2 coaxes
to read out **100 - 1000** detectors

- Reliable fabrication of 64-pixel array
- Successful characterization of first prototypes
  → optimization of design parameters

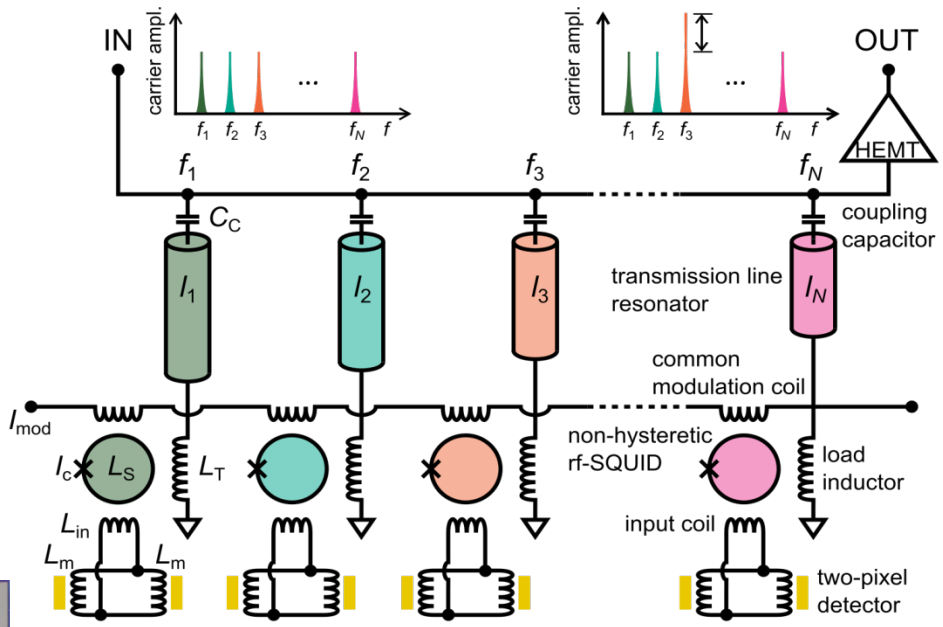

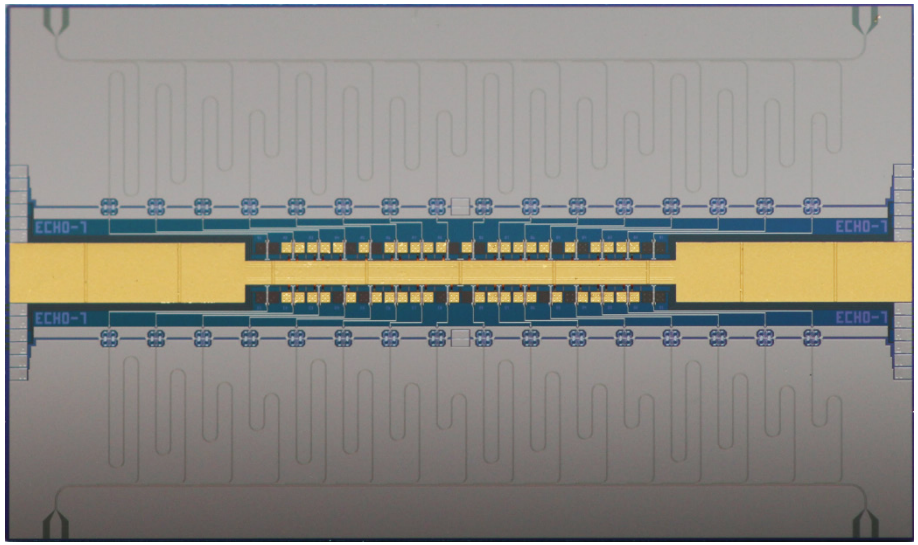

Microwave SQUID Multiplexer for the Readout of Metallic Magnetic Calorimeters
S.Kempf et al., *J. Low. Temp. Phys.* **175** (2014) 850-860

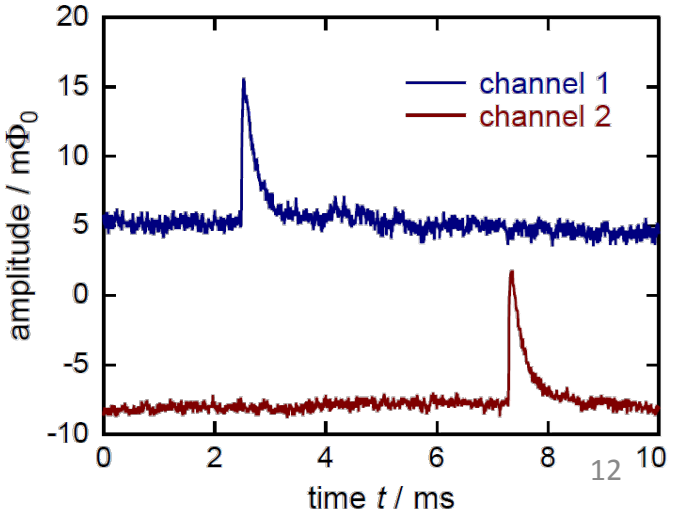

Neutrino mass determination

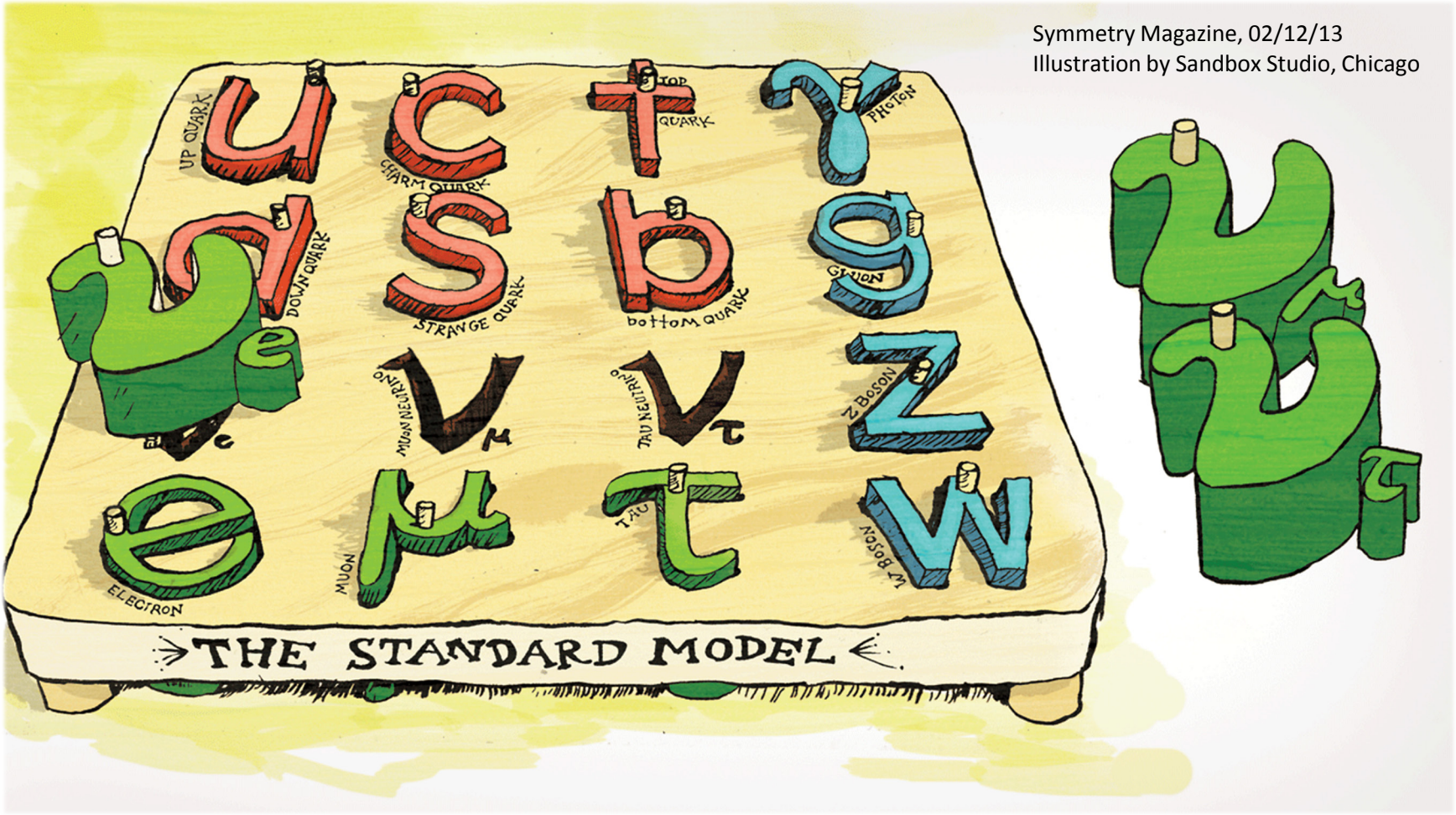

Beta decay and electron capture

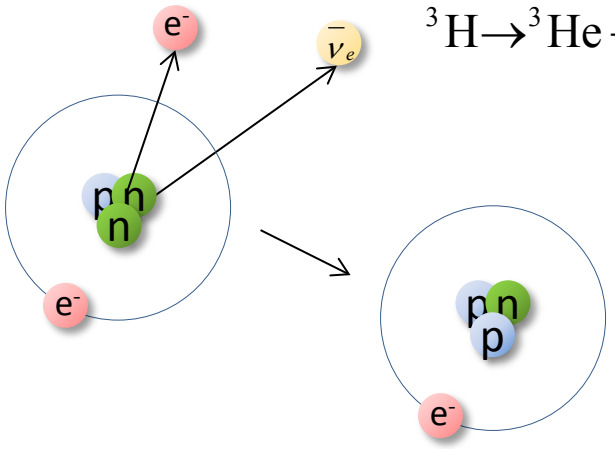

$$^{3}\mathrm{H} \rightarrow {}^{3}\mathrm{He} + e^{-} + \bar{\nu}_e$$

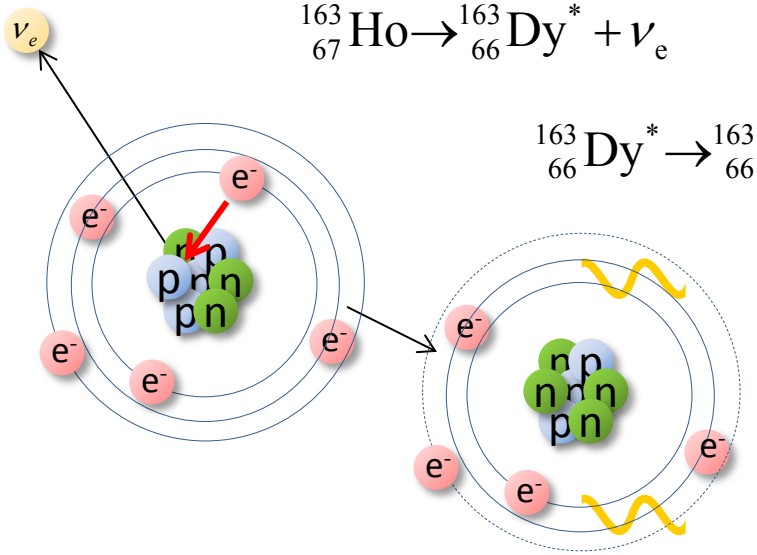

$$^{163}_{67}\mathrm{Ho} \rightarrow {}^{163}_{66}\mathrm{Dy}^{*} + \nu_e$$

$$^{163}_{66}\mathrm{Dy}^{*} \rightarrow {}^{163}_{66}\mathrm{Dy} + E_C$$

- $\tau_{1/2} \cong 12.3$ years (4*10^8 atoms for 1 Bq)
- Q_β = 18 592.01(7) eV

E.G. Myers et al., *Phys. Rev. Lett.* **114** (2015) 013003

- $\tau_{1/2} \cong 4570$ years (2*10^{11} atoms for 1 Bq)
- $Q_{EC} = (2.833 \pm 0.030^{stat} \pm 0.015^{syst})$ keV

S. Eliseev et al., *Phys. Rev. Lett.* **115** (2015) 062501

Beta decay and electron capture

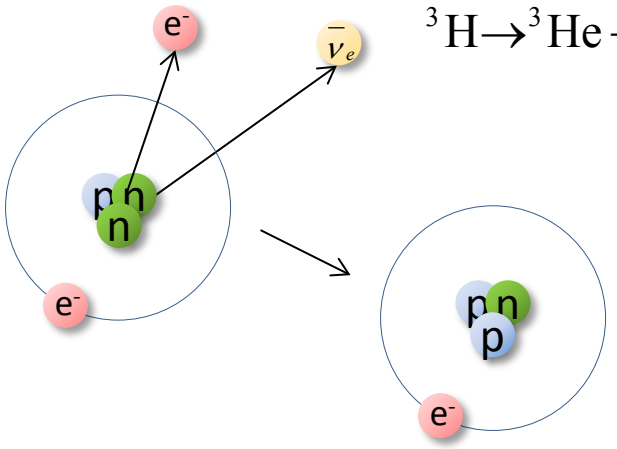

$$^{3}\mathrm{H} \rightarrow {}^{3}\mathrm{He} + e^{-} + \bar{\nu}_e$$

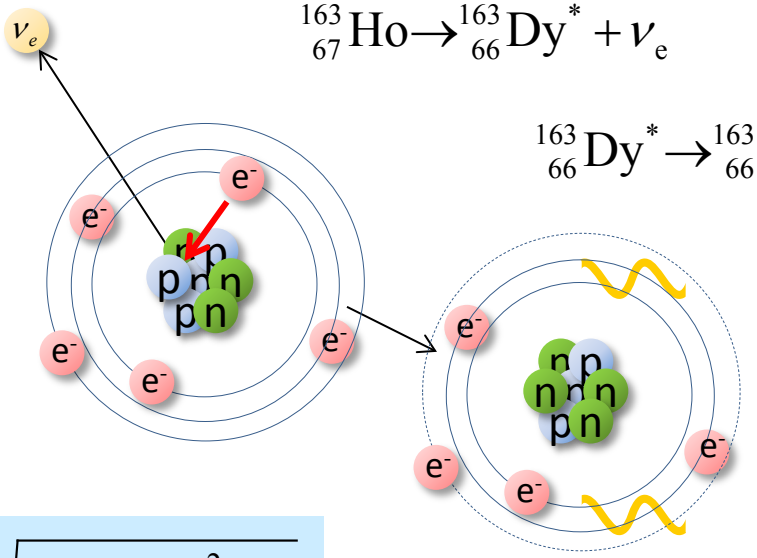

$$^{163}_{67}\mathrm{Ho} \rightarrow {}^{163}_{66}\mathrm{Dy}^{*} + \nu_e$$

$$^{163}_{66}\mathrm{Dy}^{*} \rightarrow {}^{163}_{66}\mathrm{Dy} + E_C$$

$$\frac{dW}{dE} \propto (Q - E)^2 \sqrt{1 - \frac{m_\nu^{\,2}}{(Q - E)^2}}$$

- $\tau_{1/2} \cong 12.3$ years (4*10^8 atoms for 1 Bq)
- Q_β = 18 592.01(7) eV

E.G. Myers et al., *Phys. Rev. Lett.* **114** (2015) 013003

- $\tau_{1/2} \cong 4570$ years (2*10^{11} atoms for 1 Bq)
- $Q_{EC} = (2.833 \pm 0.030^{stat} \pm 0.015^{syst})$ keV

S. Eliseev et al., *Phys. Rev. Lett.* **115** (2015) 062501

Electron capture in ^{163}Ho: spectrum

Atomic de-excitation:

- X-ray emission
- Auger electrons
- Coster-Kronig transitions

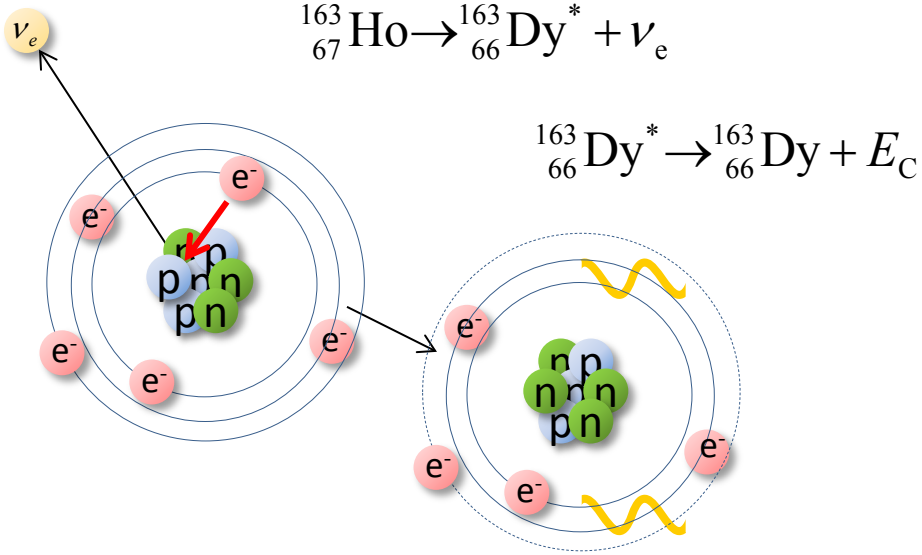

- $\tau_{1/2} \cong 4570$ years (2*10^{11} atoms for 1 Bq)
- $Q_{EC} = (2.833 \pm 0.030^{stat} \pm 0.015^{syst})$ keV

S. Eliseev et al., *Phys. Rev. Lett.* **115** (2015) 062501

Electron capture in ^{163}Ho: spectrum

Atomic de-excitation:

- **X-ray emission**
- Auger electrons
- Coster-Kronig transitions

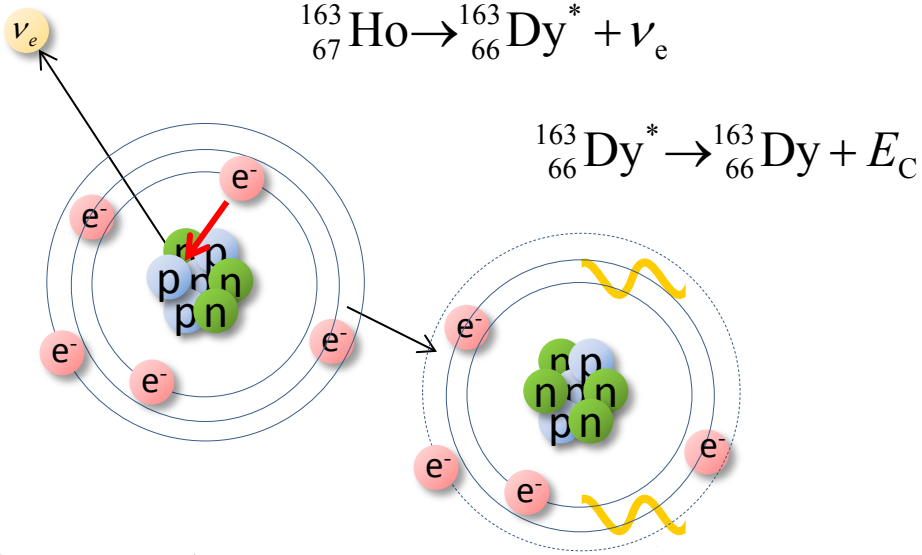

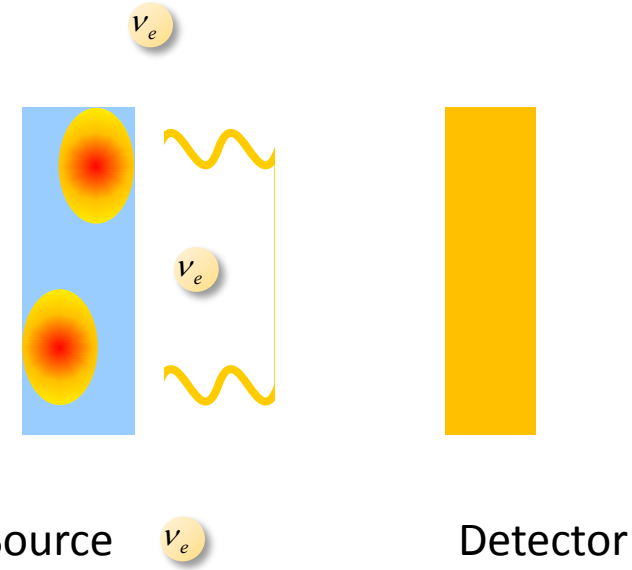

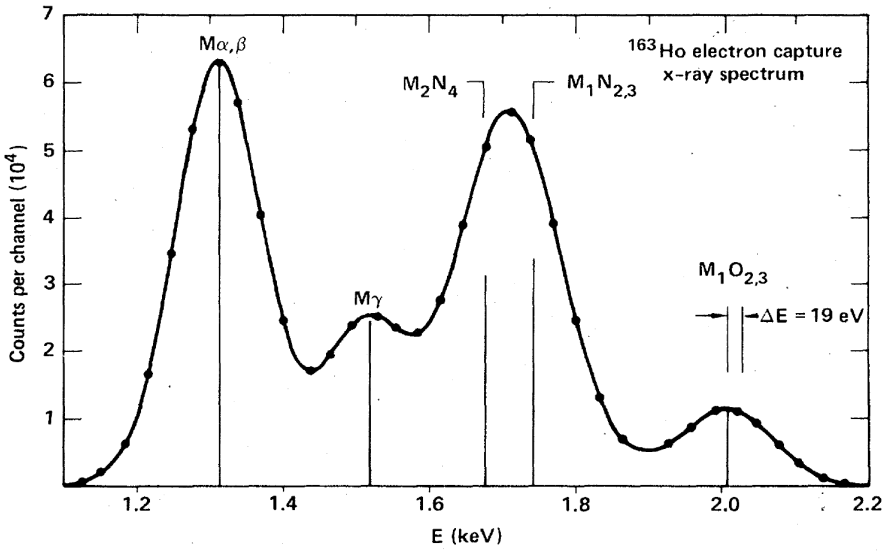

P. T. Springer, C. L. Bennett, and P. A. Baisden Phys. Rev. A 35 (1987) 679

Electron capture in ^{163}Ho: spectrum

Atomic de-excitation:

- **X-ray emission**
- Auger electrons
- Coster-Kronig transitions

$$^{163}_{67}\mathrm{Ho} \rightarrow ^{163}_{66}\mathrm{Dy}^{*} + \nu_e$$

$$^{163}_{66}\mathrm{Dy}^{*} \rightarrow ^{163}_{66}\mathrm{Dy} + E_C$$

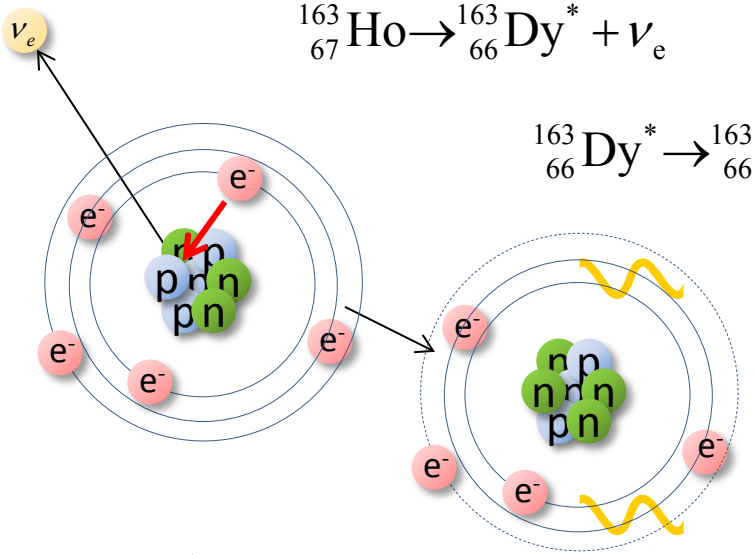

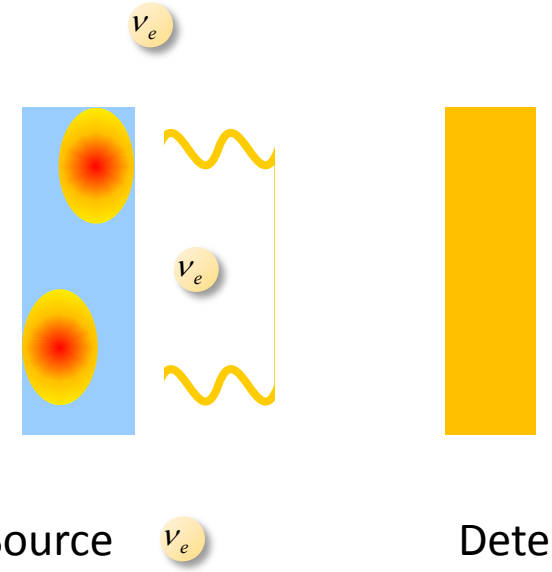

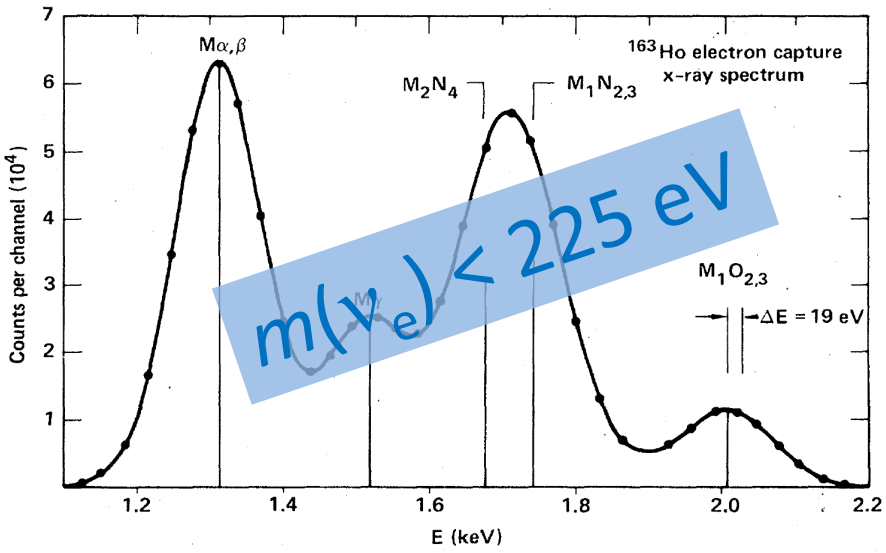

P. T. Springer, C. L. Bennett, and P. A. Baisden Phys. Rev. A 35 (1987) 679

Electron capture in ^{163}Ho: spectrum

Atomic de-excitation:

- **X-ray emission**
- **Auger electrons**
- **Coster-Kronig transitions**

Calorimetric measurement

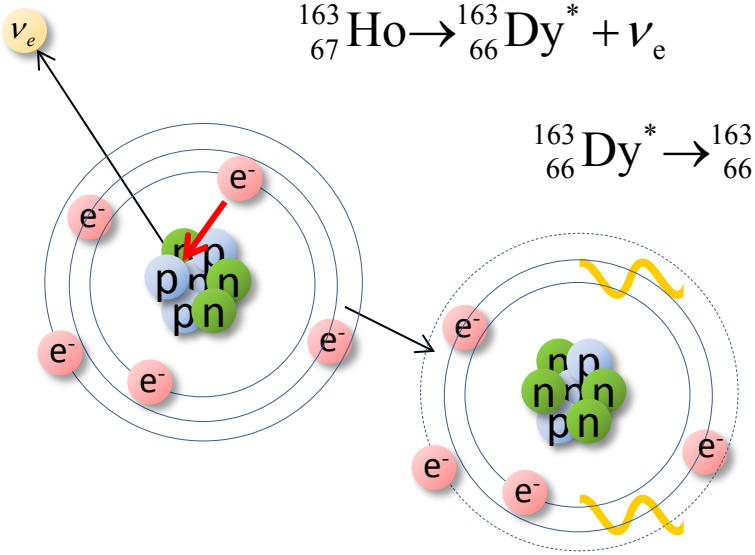

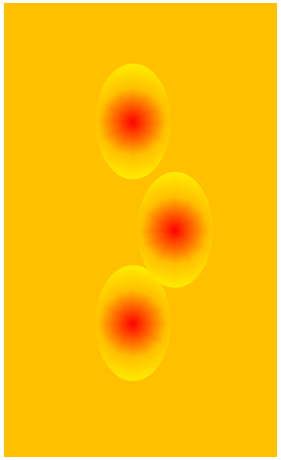

Source = Detector

A. De Rujula and M. Lusignoli, *Phys. Lett.* **118B** (1982)

Electron capture in ^{163}Ho: spectrum

Atomic de-excitation:

- **X-ray emission**
- **Auger electrons**
- **Coster-Kronig transitions**

Calorimetric measurement

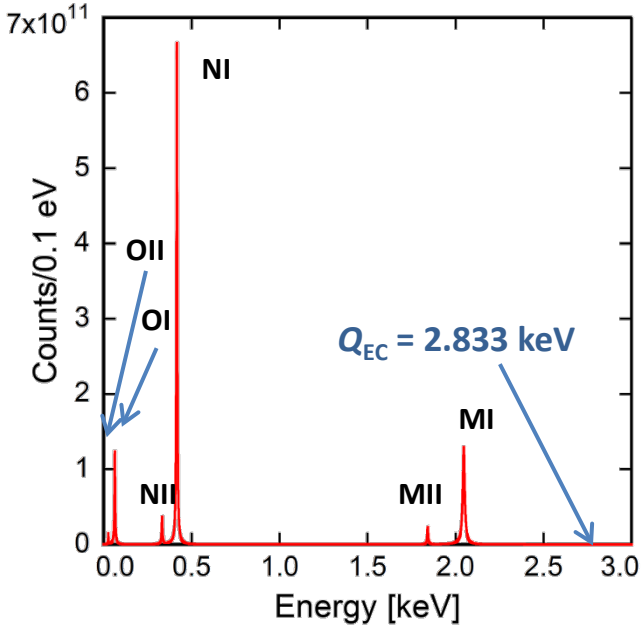

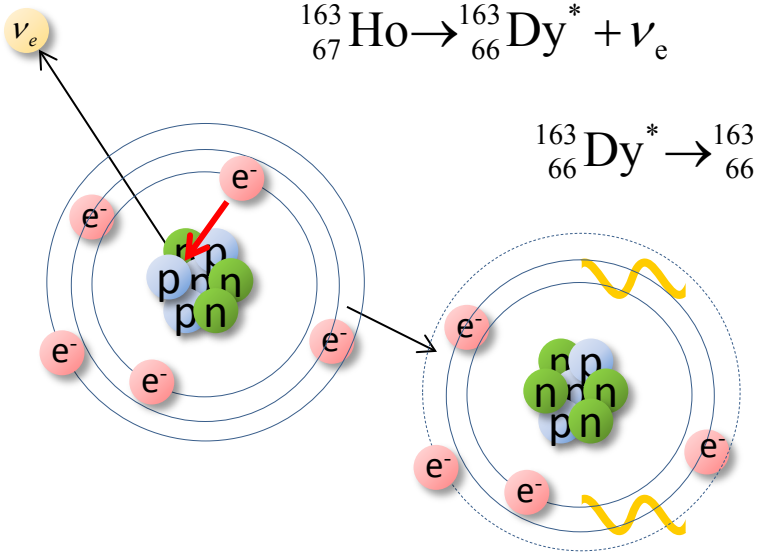

$$^{163}_{67}\mathrm{Ho} \rightarrow ^{163}_{66}\mathrm{Dy}^{*} + \nu_e$$

$$^{163}_{66}\mathrm{Dy}^{*} \rightarrow ^{163}_{66}\mathrm{Dy} + E_C$$

$$\frac{dW}{dE_C} = \mathrm{A}(Q_{EC} - E_C)^2 \sqrt{1 - \frac{m_\nu^{\,2}}{(Q_{EC} - E_C)^2}} \sum_H B_H \varphi_H^{\,2}(0) \frac{\frac{\Gamma_H}{2\pi}}{(E_C - E_H)^2 + \frac{\Gamma_H^{\,2}}{4}}$$

Electron capture in ^{163}Ho: spectrum

Atomic de-excitation:

- **X-ray emission**
- **Auger electrons**
- **Coster-Kronig transitions**

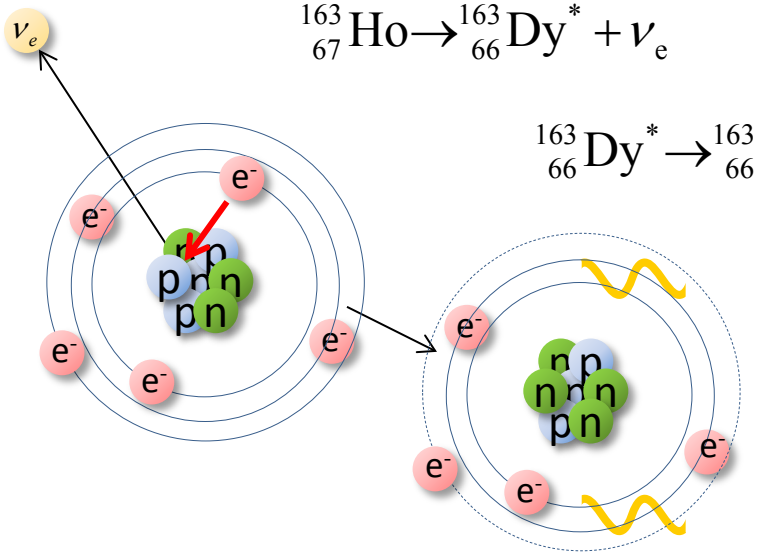

Calorimetric measurement

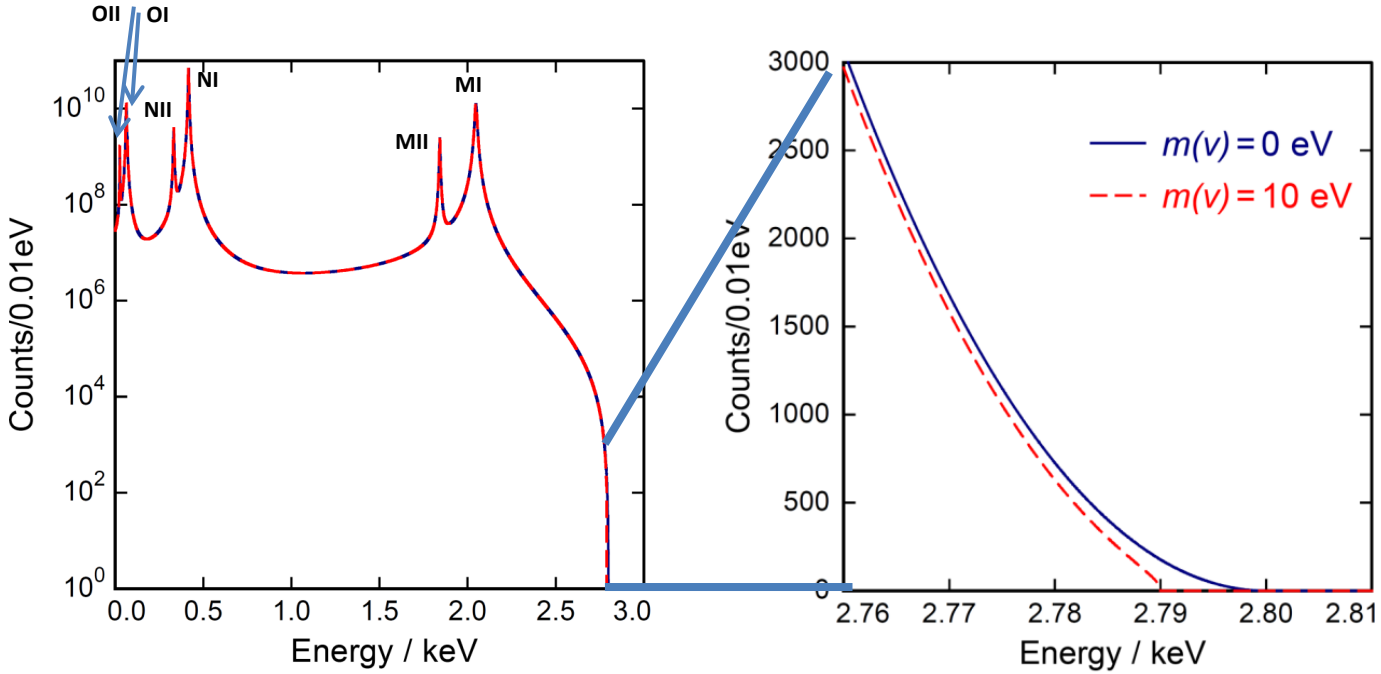

Requirements for sub-eV sensitivity in ECHo

Statistics in the end point region

- $N_{ev} > 10^{14}$ → **A ≈ 1 MBq**

Unresolved pile-up ($f_{pu} \sim a \cdot \tau_r$)

- f_{pu} **< 10^{-5}**
- τ_r < 1 µs → a ~ 10 Bq
- 10^5 pixels

Precision characterization of the endpoint region

- **ΔE_{FWHM} < 3 eV**

Background level

- **< 10^{-6} events/eV/det/day**

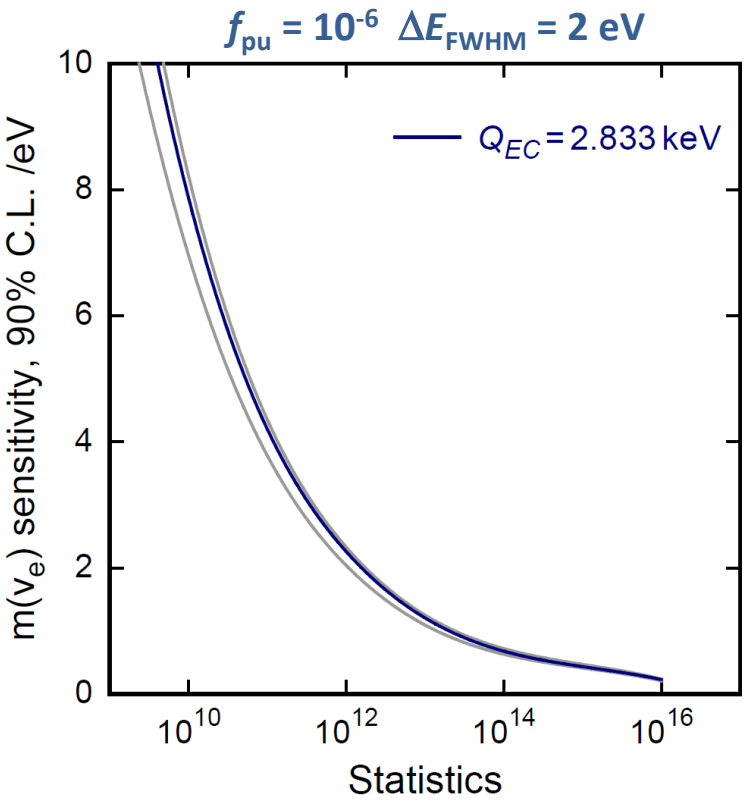

^{163}Ho high purity source

Required activity in the detectors: Final experiment → >10^6 Bq → >10^{17} atoms

- Neutron irradiation

  (n,γ)-reaction on ^{162}Er

  High cross-section

  Radioactive contaminants

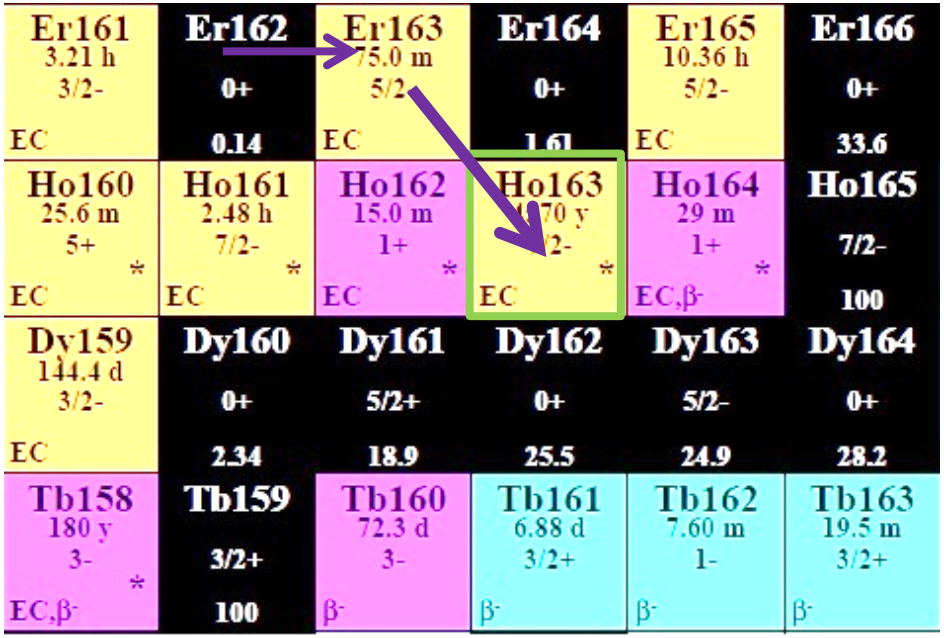

H. Dorrer et al, Radiochim. Acta (2018)

^{163}Ho high purity source

Required activity in the detectors: Final experiment → >10^6 Bq → >10^{17} atoms

- Neutron irradiation

  (n,γ)-reaction on ^{162}Er

High cross-section 

Radioactive contaminants  → Excellent chemical separation

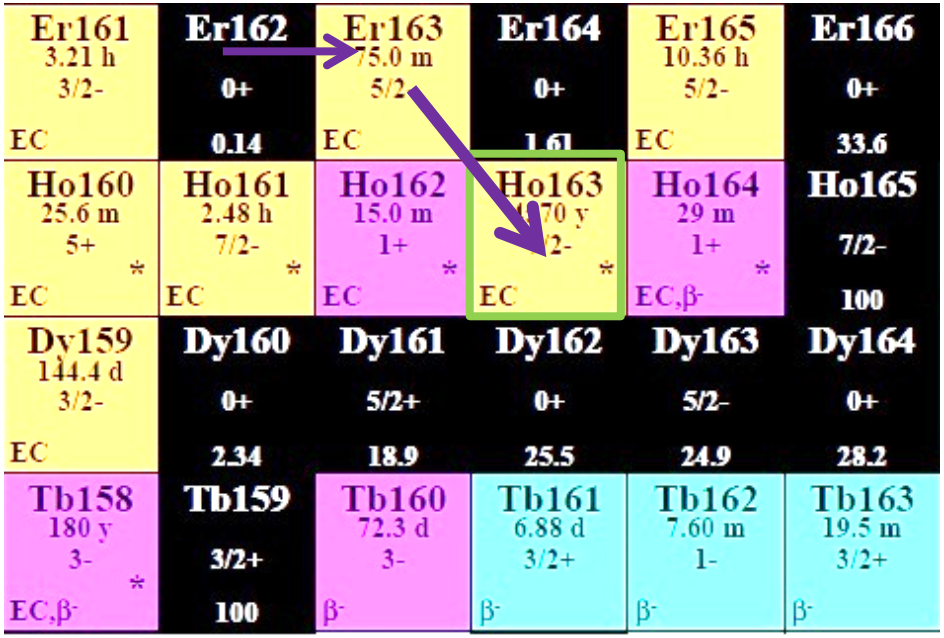

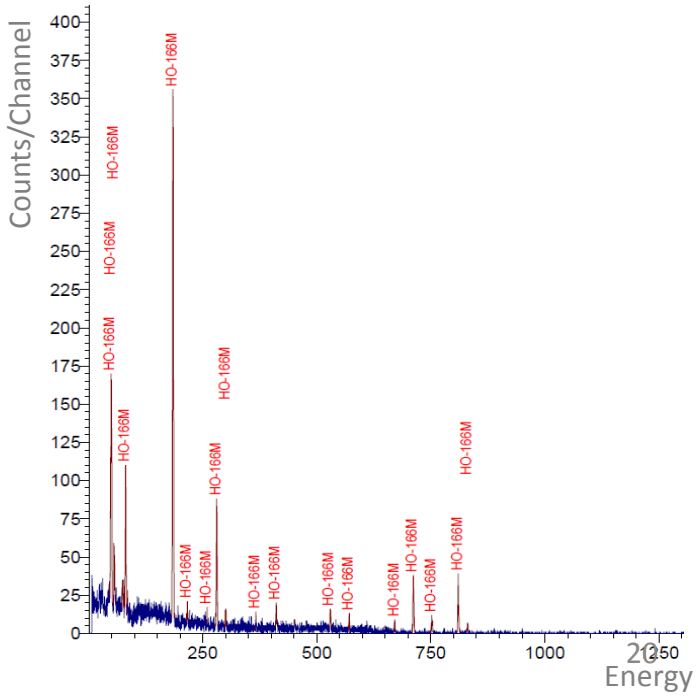

H. Dorrer et al, Radiochim. Acta (2018)

Mass separation and ^{163}Ho ion-implantation

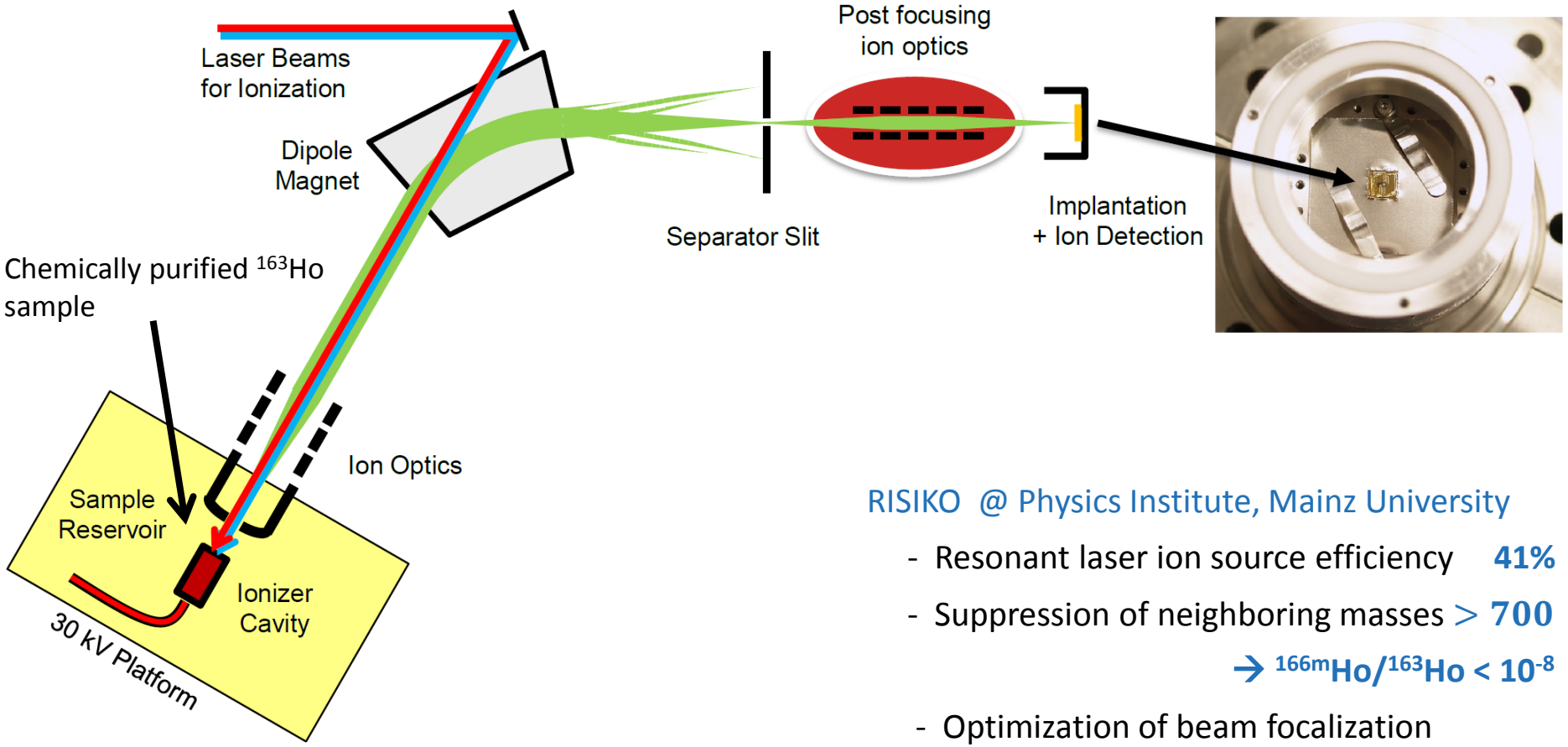

RISIKO @ Physics Institute, Mainz University

- Resonant laser ion source efficiency **41%**
- Suppression of neighboring masses $>$ **700**

→ **^{166m}Ho/^{163}Ho < 10^{-8}**

- Optimization of beam focalization

F. Schneider et al ., *NIM B* **376** (2016) 388

ECHo-1k array

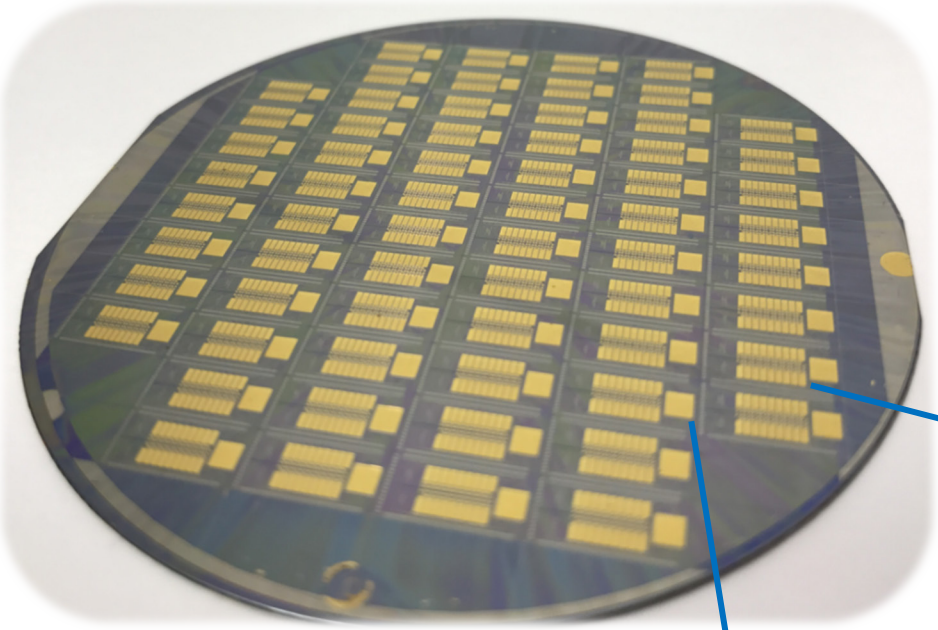

3“ wafer with 64 ECHo-1k chip

Suitable for
parallel and multiplexed readout

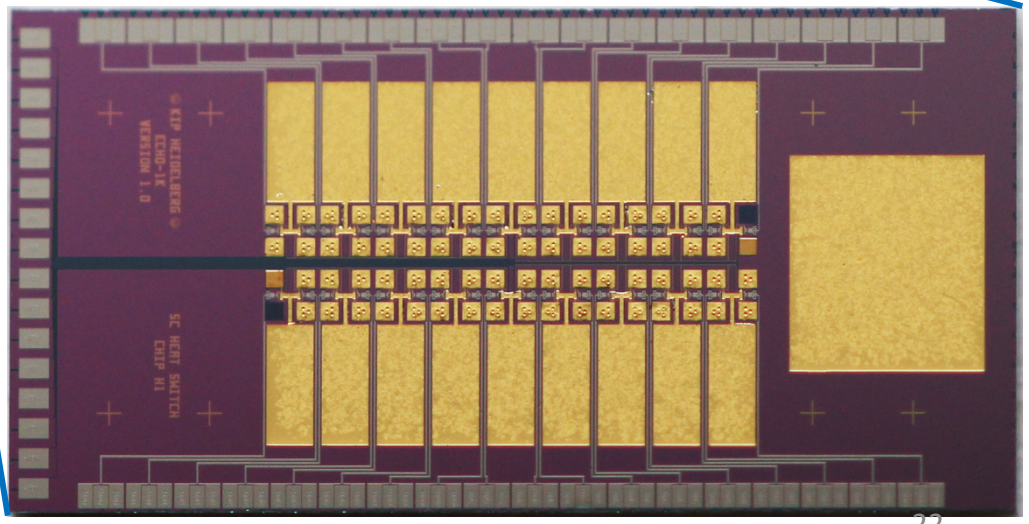

64 pixels which can be loaded with ^{163}Ho
+ 4 detectors for diagnostics

Design performance:
ΔE_{FWHM} ~ 5 eV
τ_r ~ 90 ns (single channel readout)
τ_r ~ 300 ns (multiplexed read-out)

S.Kempf *et al., J. Low. Temp. Phys*. **176** (2014) 426

ECHo-1k array

100% of the chips selected at RT have good performance at low temperature

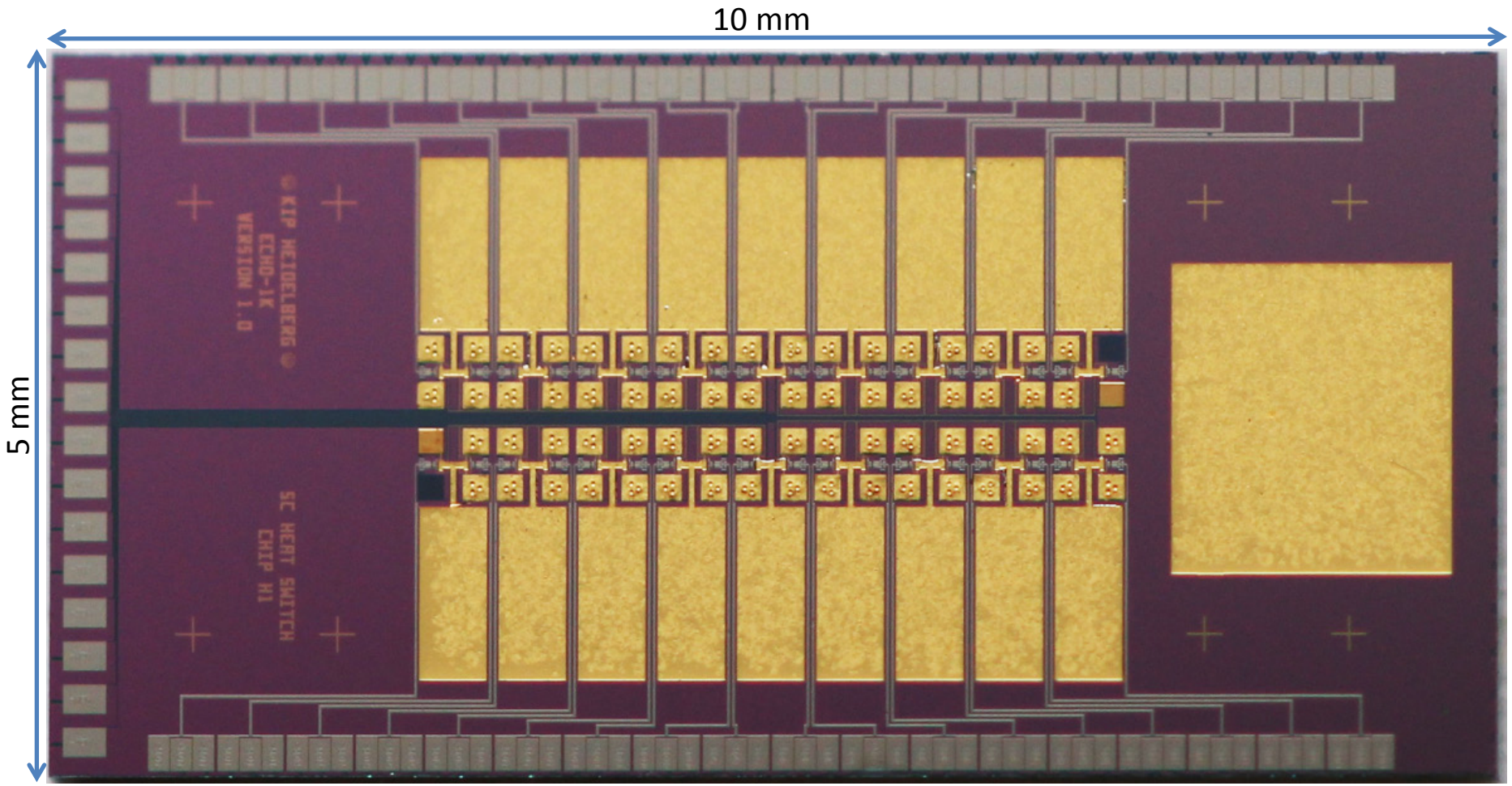

ECHo-1k array

high geometrical efficiency for ^{163}Ho implantation

presence of non-implanted chips for in-situ background determination

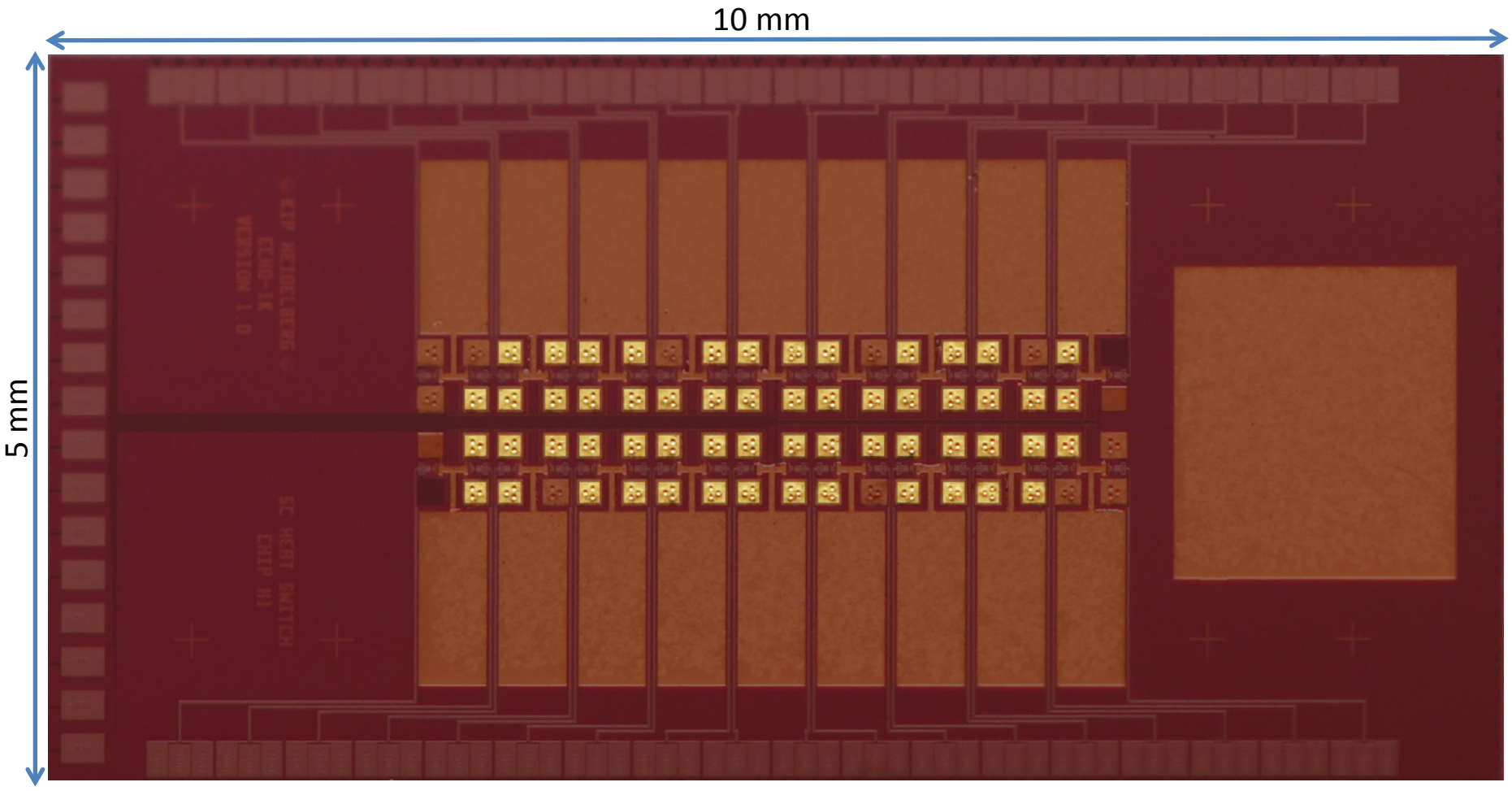

Background in ECHo

Background sources:

- Radioactivity in the detector
- Environmental radioactivity → Material screening
- Cosmic rays → Underground labs, μ-Veto
  Induced secondary radiation

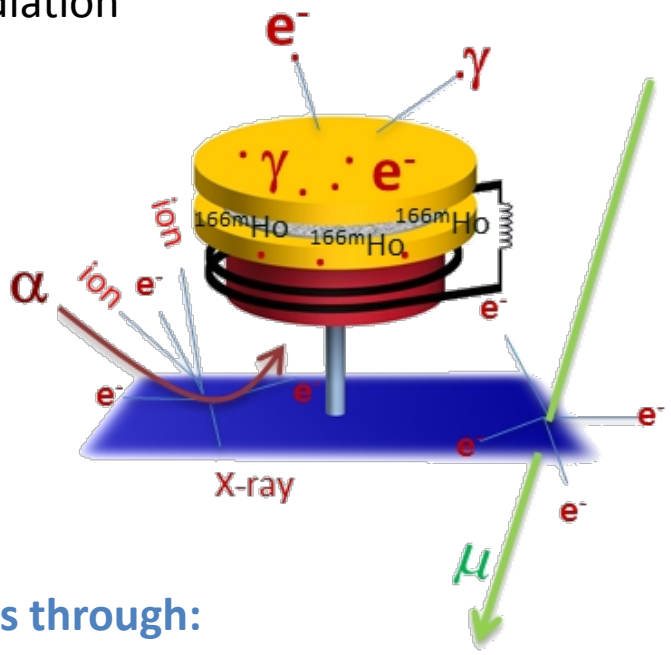

Study of background sources through:

- Monte Carlo simulations
- Dedicated experiments

Screening facilities
- Uni-Tübingen
- **Felsenkeller**

ECHo cryogenic platform

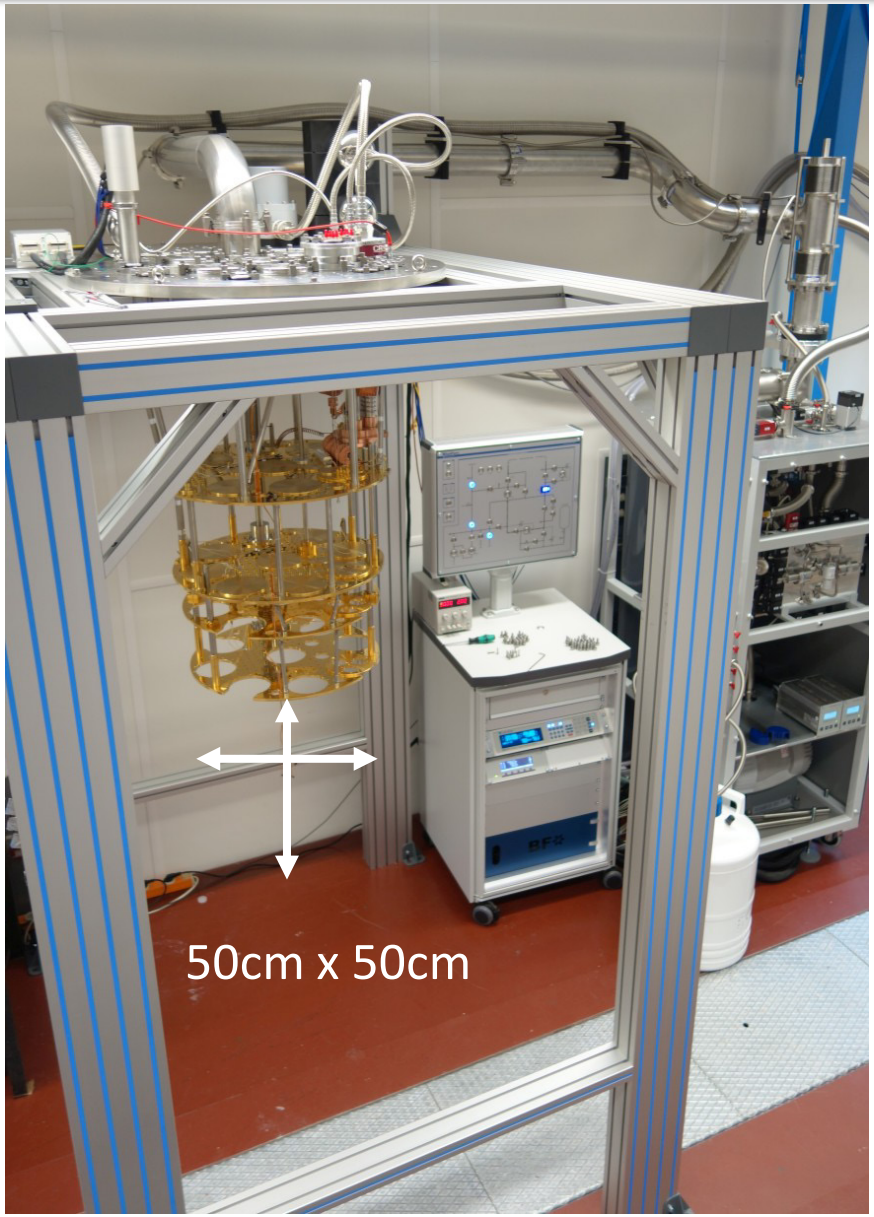

- Large space at MXC enough for several ECHo phases
- cooling power: 15µW @ 20 mK
- Possibility to load 200kg for passive shielding

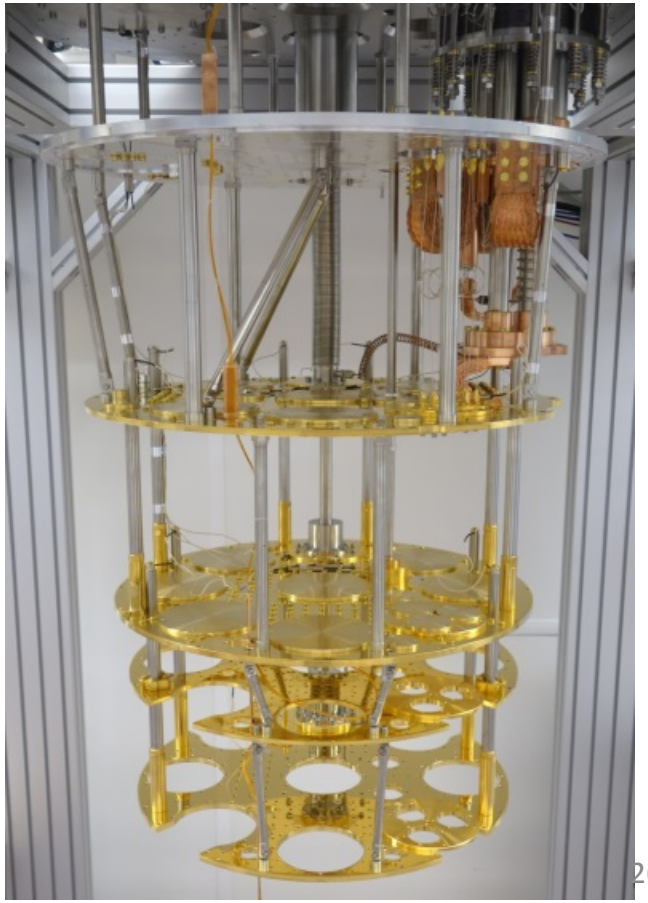

ECHo-1k set-up

- ECHo-1k chip implanted at RISIKO Uni-Mainz

  → ^{163}Ho activity $A \approx 2$ Bq

- 4 Front-end chips each with 8 dc-SQUIDs

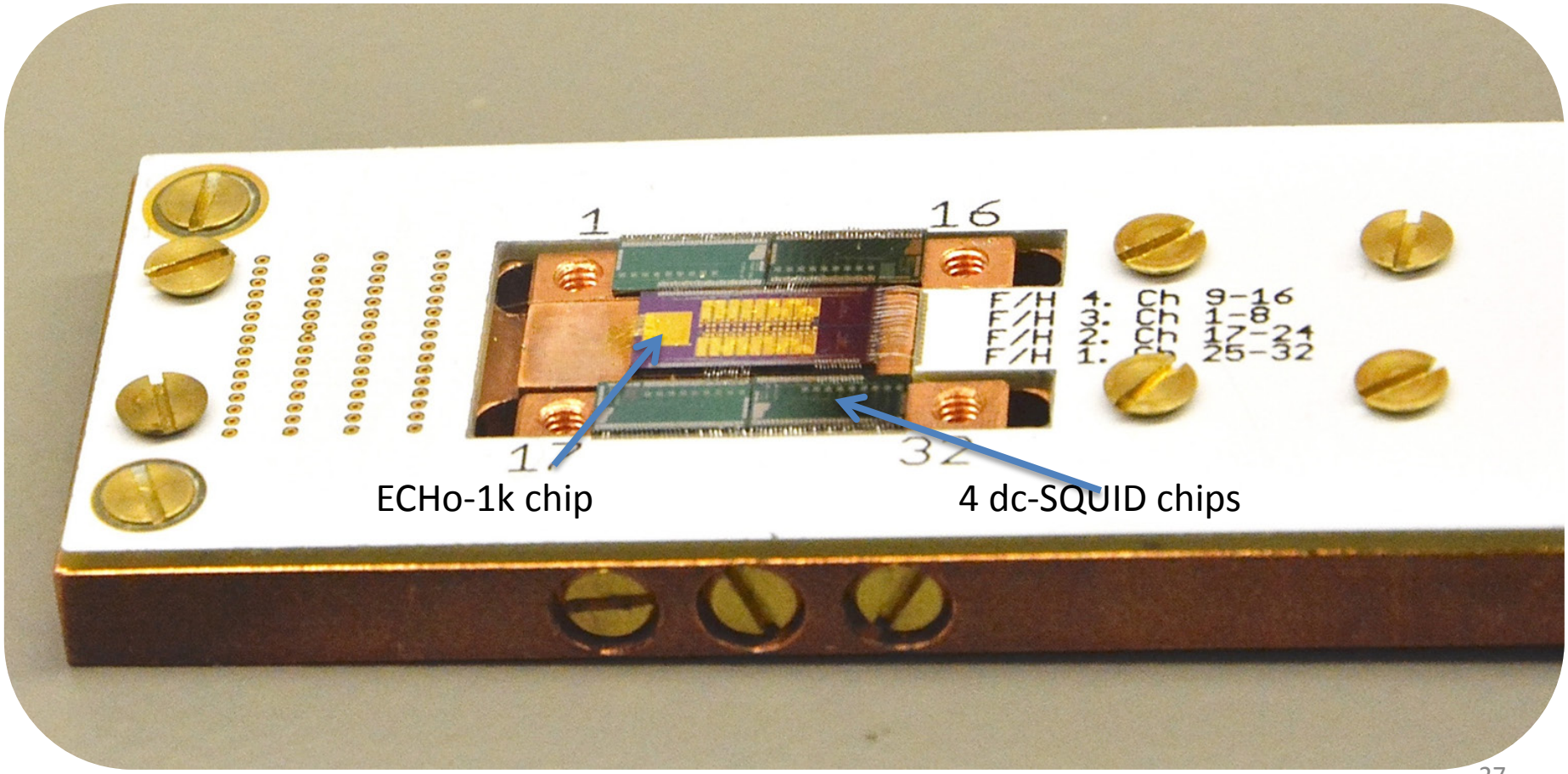

ECHo-1k set-up

- Circuit board designed for the ECHo-1k experiment

  →Parallel read-out of 64 pixels

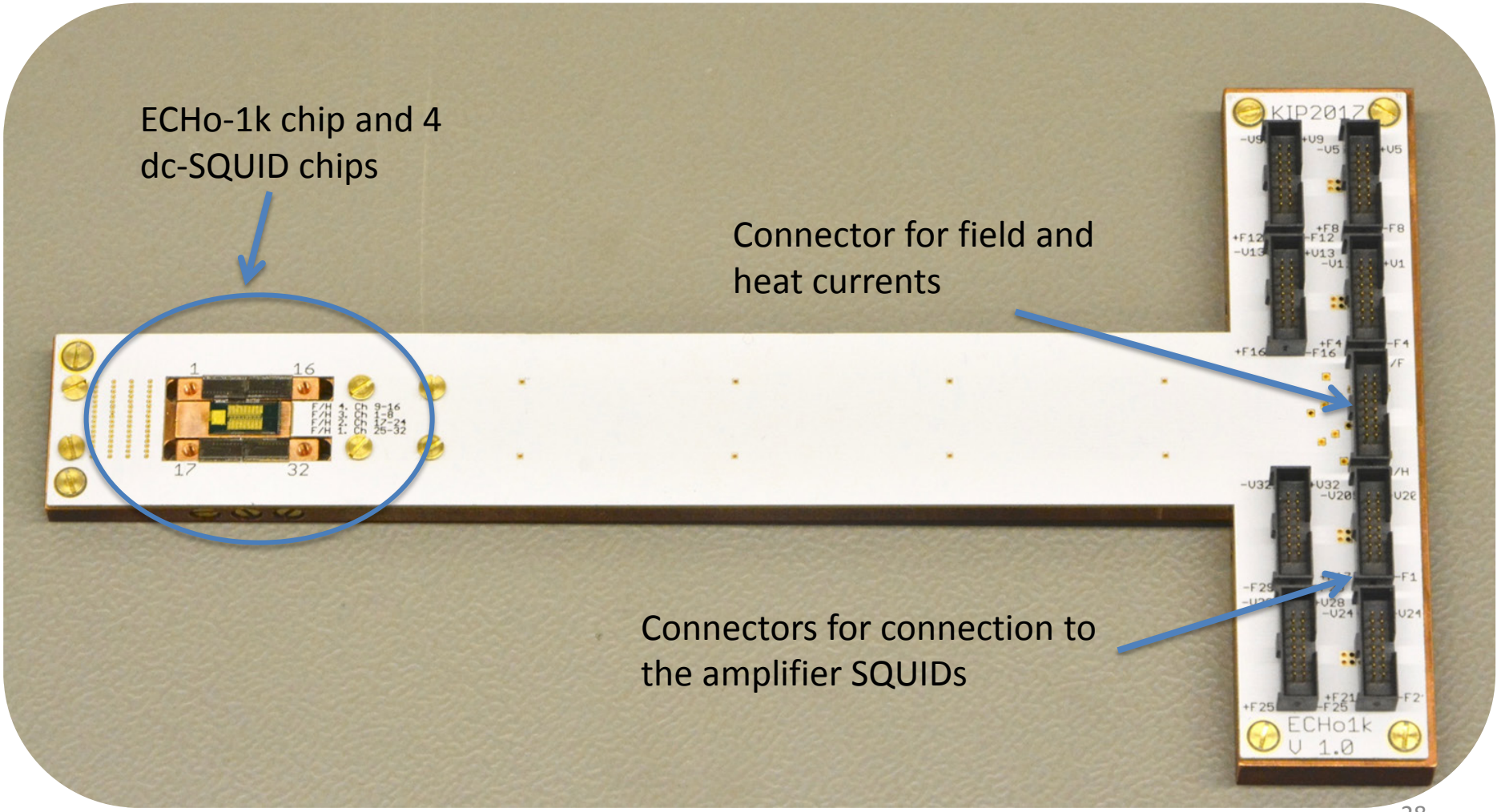

ECHo-1k set-up

Aluminum superconducting shield

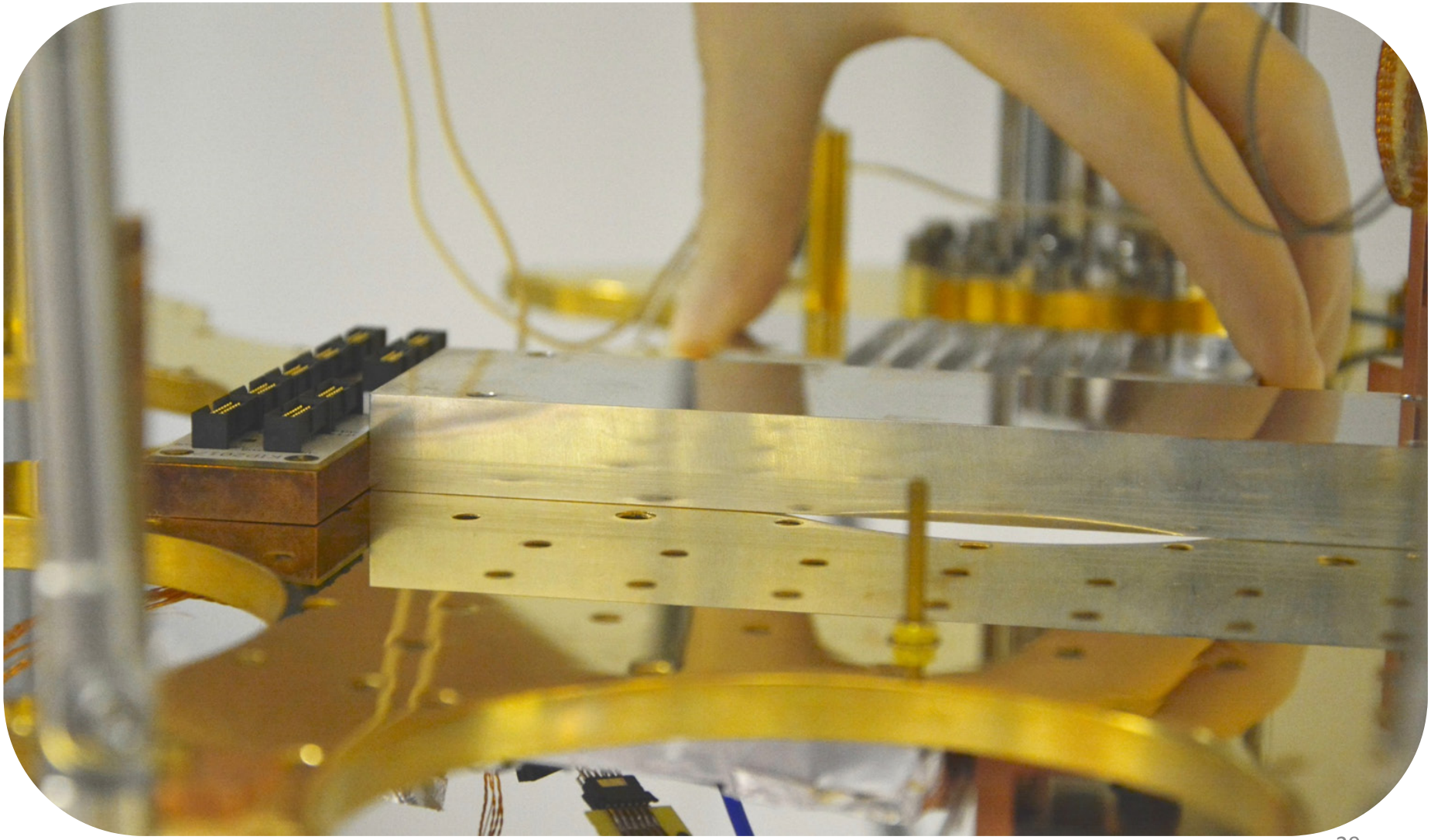

ECHo-1k set-up

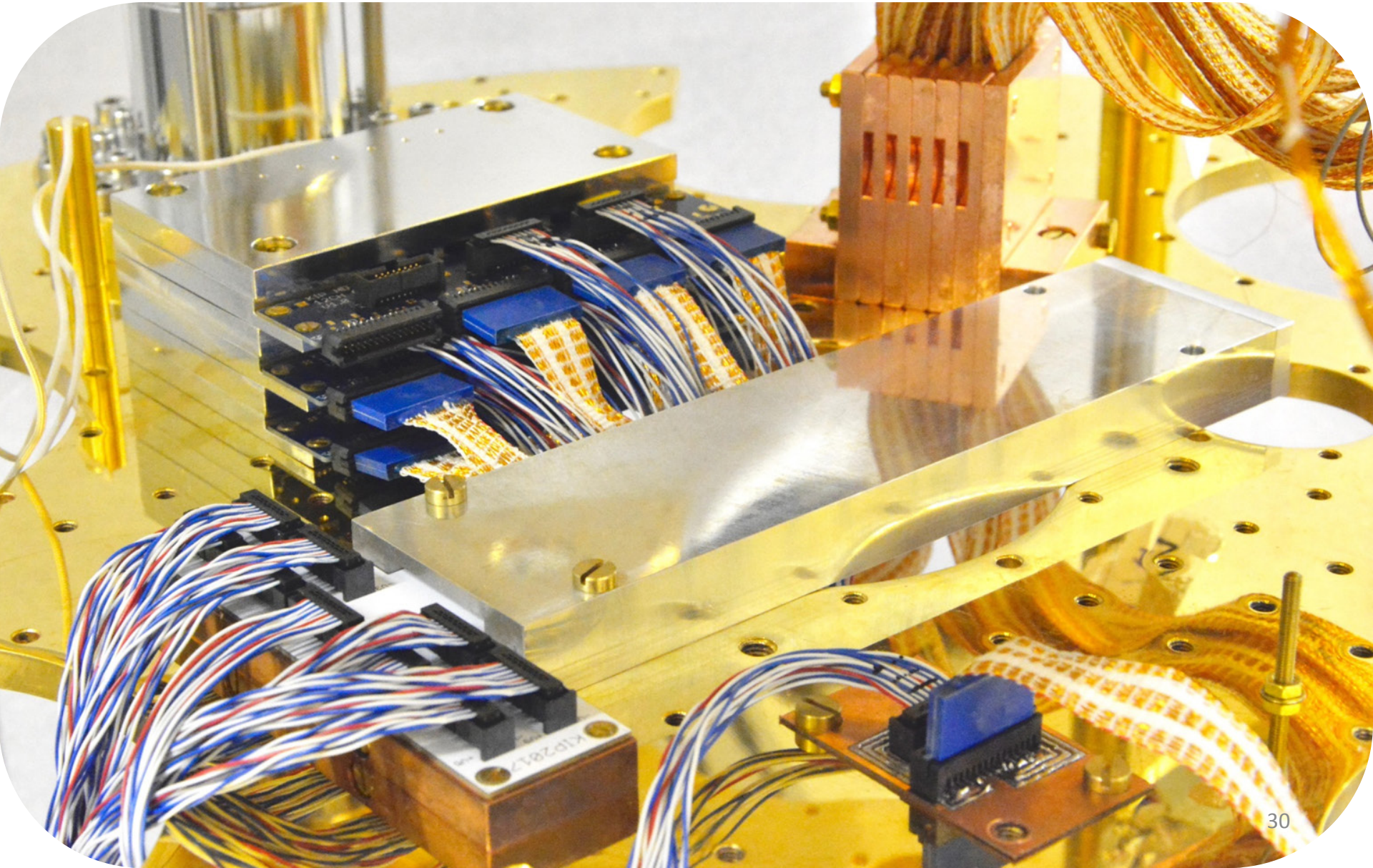

ECHo-1k: first characterization

Spectra for each pixel are separately analysed for:

- activity
- energy resolution
- calibration

Overlay 20 spectra

Presently about 30 million events

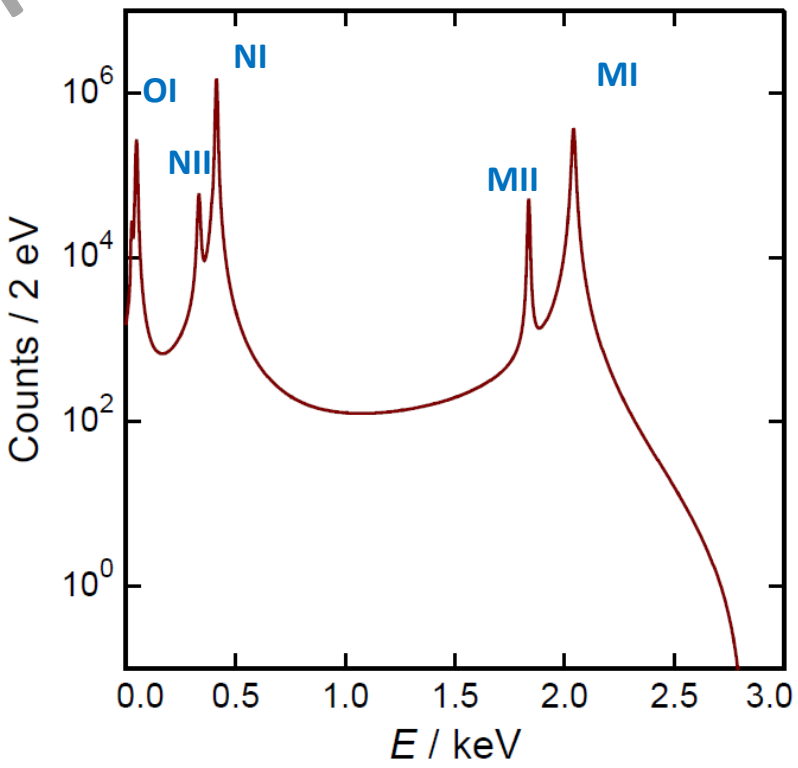

^{163}Ho spectral shape

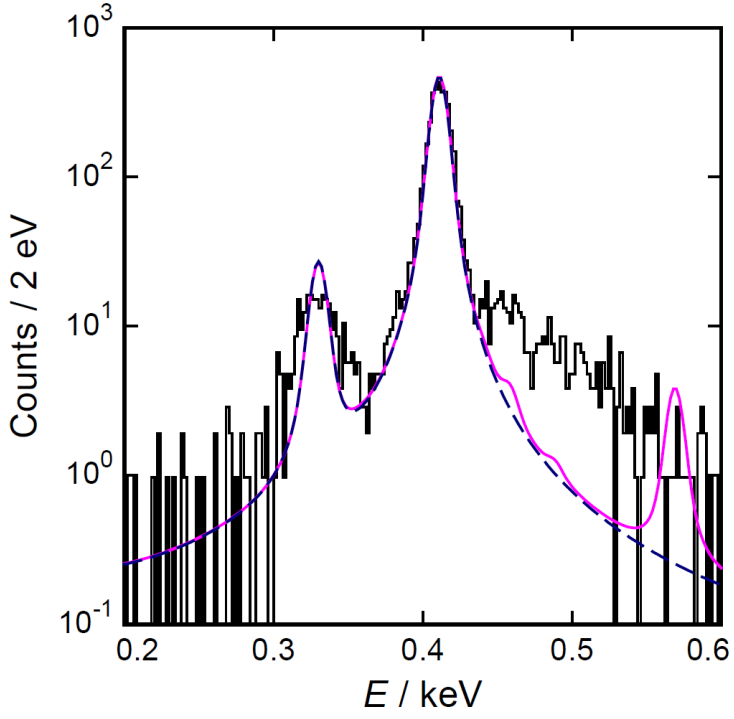

No good agreement between experimental spectrum and theory

- A. Faessler and F. Simkovic
  Phys. Rev. C **91**, 045505 (2015)
- A. De Rujula and M. Lusignoli
  JHEP 05 (2016) 015, arXiv:1601.04990v1
- A. Faessler et al.
  J. Phys. G **42** (2015) 015108
- R. G. H. Robertson
  Phys. Rev. C **91**, 035504 (2015)
- A. Faessler et al.
  Phys. Rev. C **91**, 064302 (2015)
- A. Faessler et al.
  Phys. Rev. C **95**, (2017) 045502

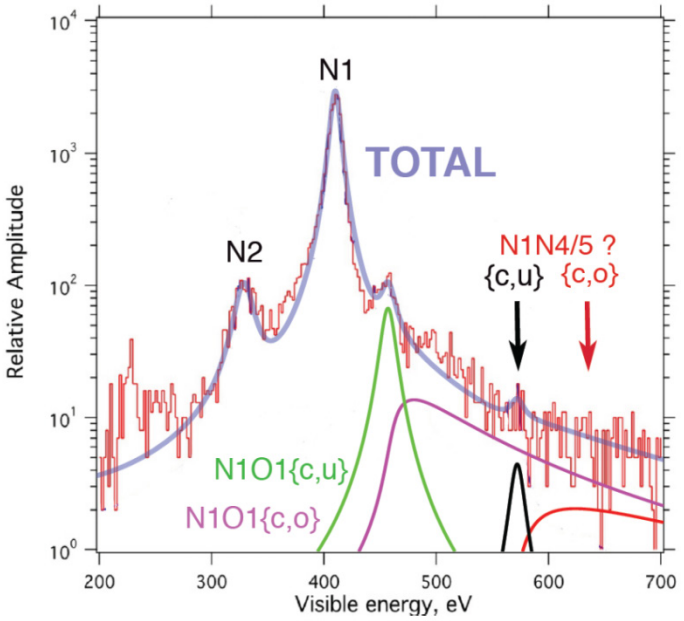

^{163}Ho spectral shape

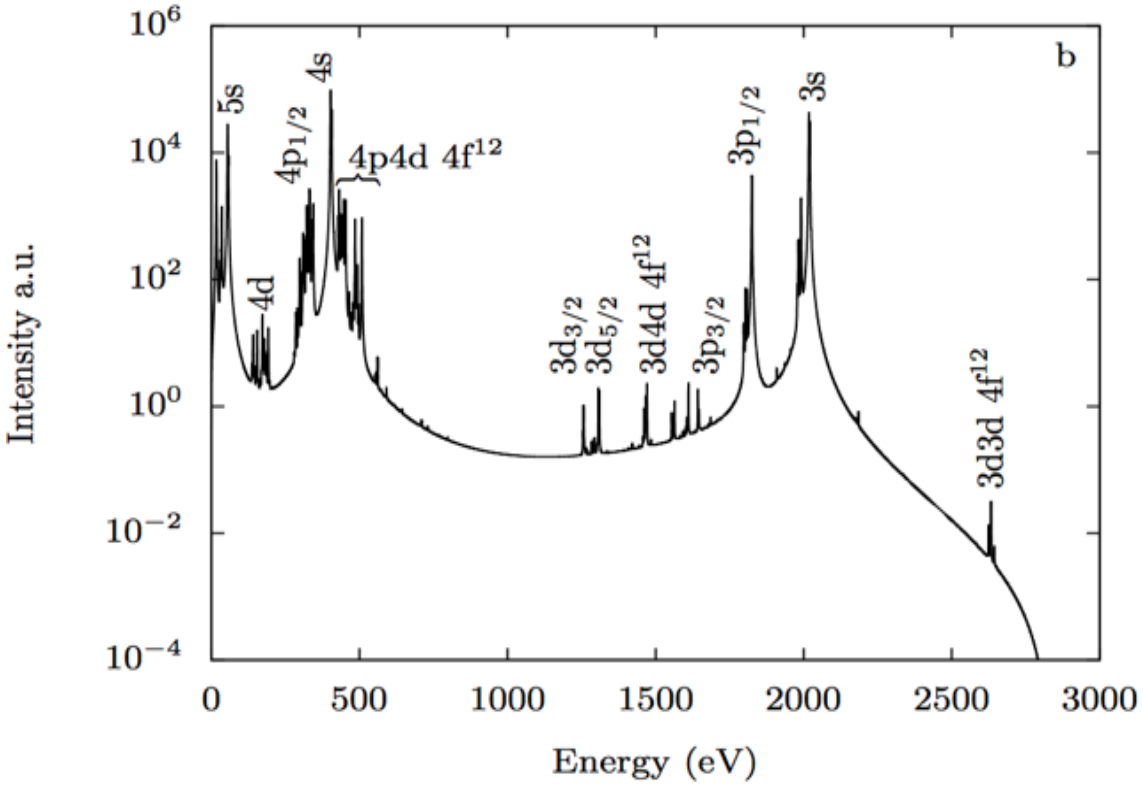

New approach

Ab inito calculation of the ^{163}Ho electron capture spectrum

Brass et al., https://arxiv.org/abs/1711.10309

Restricted to bound-states only, i.e. the spectrum is given by a finite number of resonances

→ Include decay to the continuum states
→ Study the effect of metallic host

^{163}Ho Q_{EC} Determination

$$Q_{EC} = m(^{163}\mathrm{Ho}) - m(^{163}\mathrm{Dy})$$

Penning Trap Mass Spectroscopy

@TRIGA TRAP (Uni-Mainz) (♦)

@SHIPTRAP (GSI – Darmstadt) (♦♦)

$$Q_{EC} = (2.833 \pm 0.030^{stat} \pm 0.015^{syst})\ \mathrm{keV}$$

Perfect agreement with Q_{EC} from ^{163}Ho spectrum (♣)

$$Q_{EC} = (2.858 \pm 0.010^{stat} \pm 0.05^{syst})\ \mathrm{keV}$$

$$\nu_c = \frac{qB}{m}$$

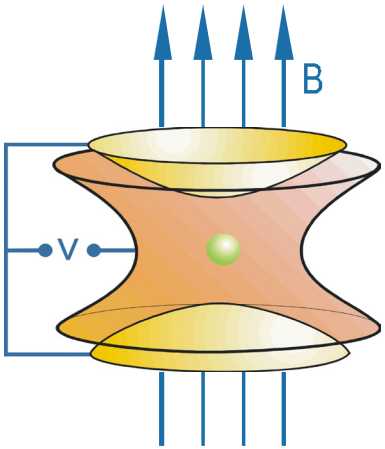

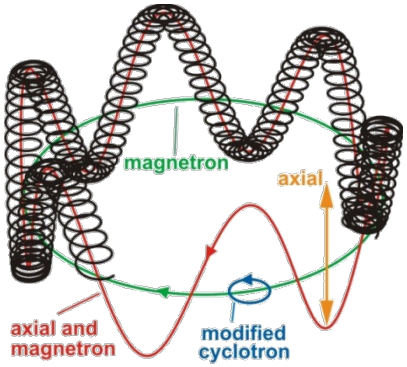

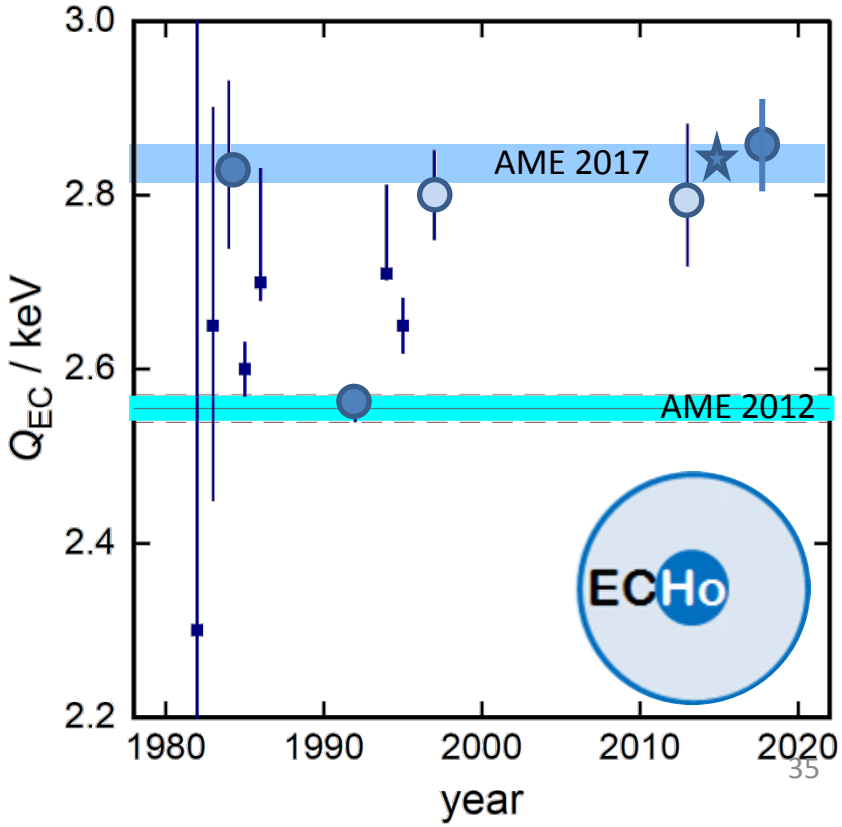

(♦) F. Schneider et al., Eur. Phys. J. A **51** (2015) 89

(♦♦) S. Eliseev et al., *Phys. Rev. Lett.* **115** (2015) 062501

(♣) P. C.-O. Ranitzsch et al., PRL 119 (2017) 122501

^{163}Ho Q_{EC} Determination

$$Q_{EC} = m(^{163}\mathrm{Ho}) - m(^{163}\mathrm{Dy})$$

Penning Trap Mass Spectroscopy

@TRIGA TRAP (Uni-Mainz)

@SHIPTRAP (GSI – Darmstadt)

$$\nu_c = \frac{qB}{m}$$

$Q_{EC} = (2.833 \pm 0.030^{stat} \pm 0.015^{syst})$ keV

Perfect agreement with Q_{EC} from ^{163}Ho spectrum

$Q_{EC} = (2.858 \pm 0.010^{stat} \pm 0.05^{syst})$ keV

Future goal: 1 eV precision

PENTATRAP @MPIK, Heidelberg (D) (*)

CHIP-TRAP @CMU Mount Pleasant (US) (**)

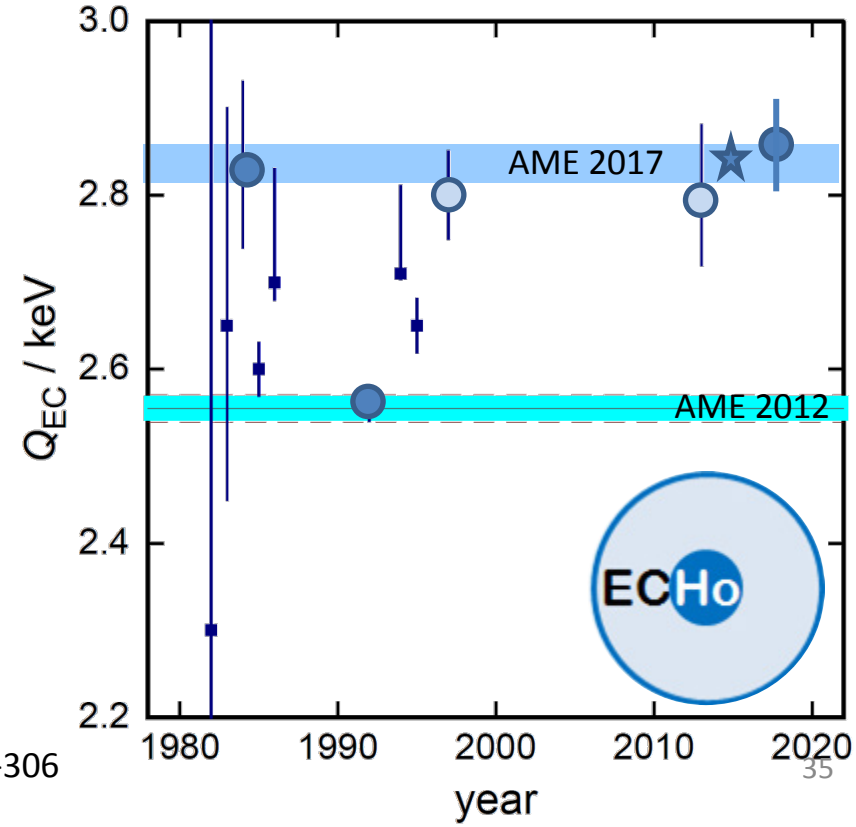

(*) J. Repp et al., Appl. Phys. B 107 (2012) 983

(*) C. Roux et al., Appl. Phys. B 107 (2012) 997

(**) M. Redshaw et al Nucl.Instrum.Meth. B376 (2016) 302-306

Sensitivity of the ECHo experiment

ECHo-1k – revised (2015 – 2018)

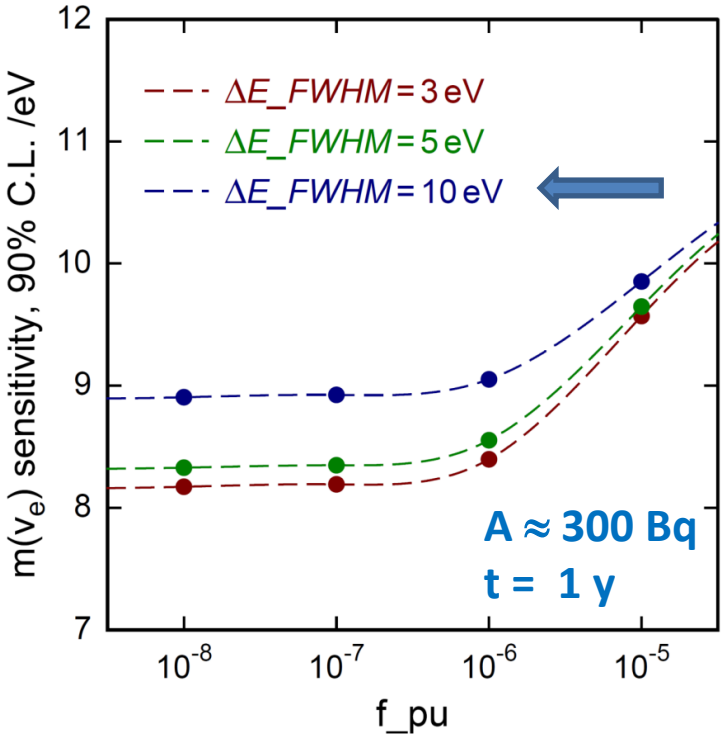

$m(\nu_e) < 10$ eV 90% C.L.

Activity per pixel 5 Bq
Number of detectors 60
Readout: parallel two stage SQUID

ECHo-100k (2018 – 2021)

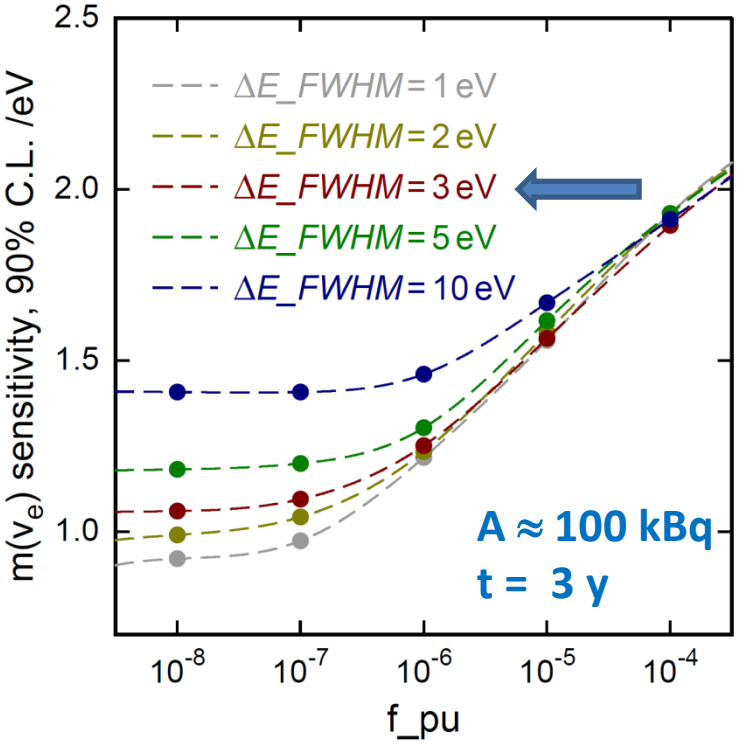

$m(\nu_e) < 1.5$ eV 90% C.L.

Activity per pixel 10 Bq
Number of detectors 12000
Readout: microwave SQUID multiplexing

Supported by DFG Research Unit FOR 2022/1

Supported by DFG Research Unit FOR 2022/2

Sterile neutrinos and ^{163}Ho

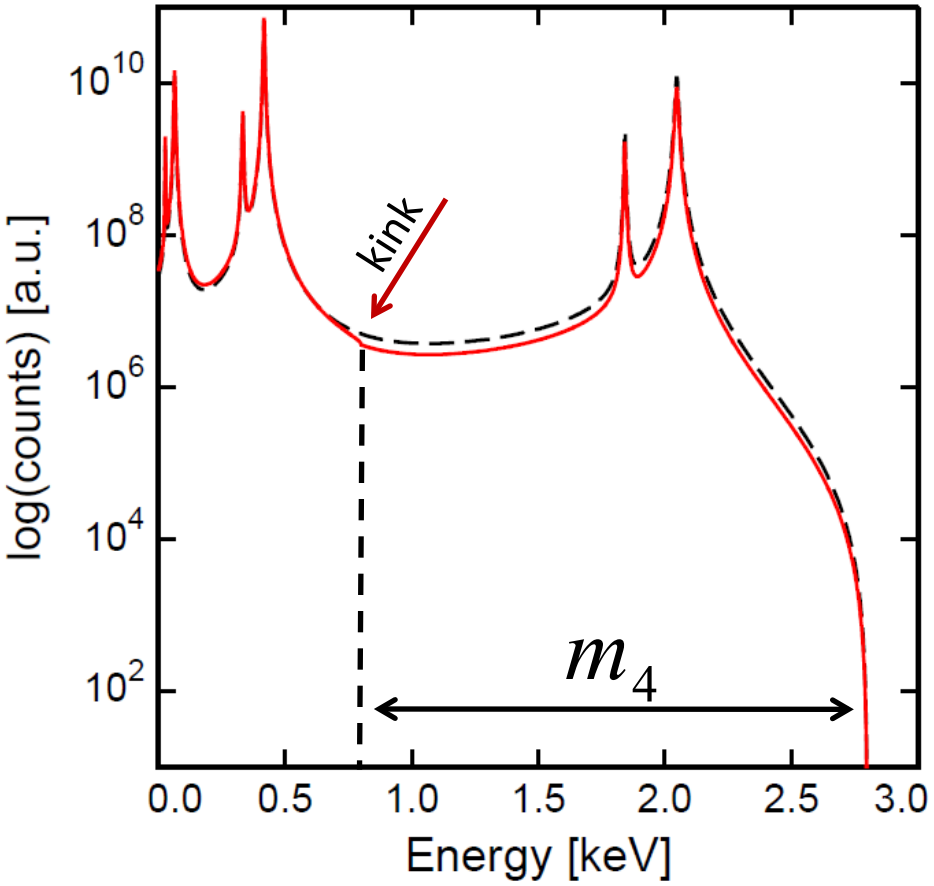

- postion of kink => m_4
- depth of kink => $|U_{e4}|^2$

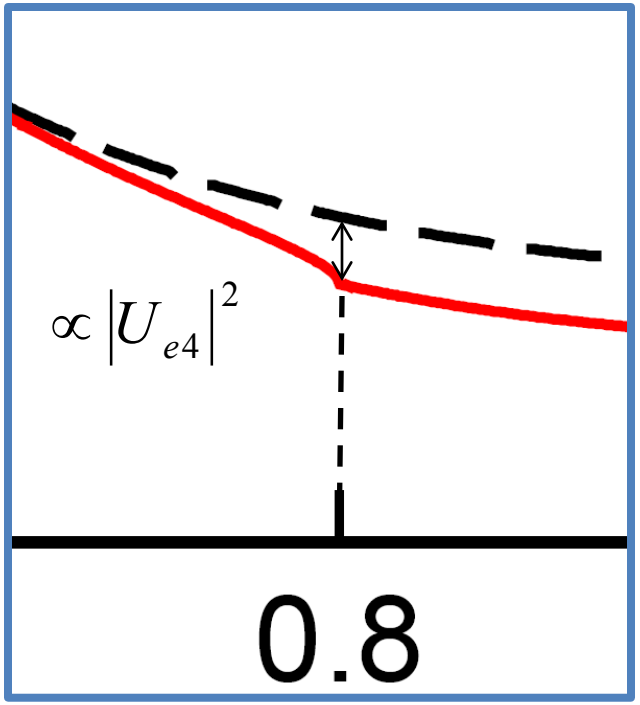

Sterile neutrinos search in ECHo

eV-scale sterile neutrinos

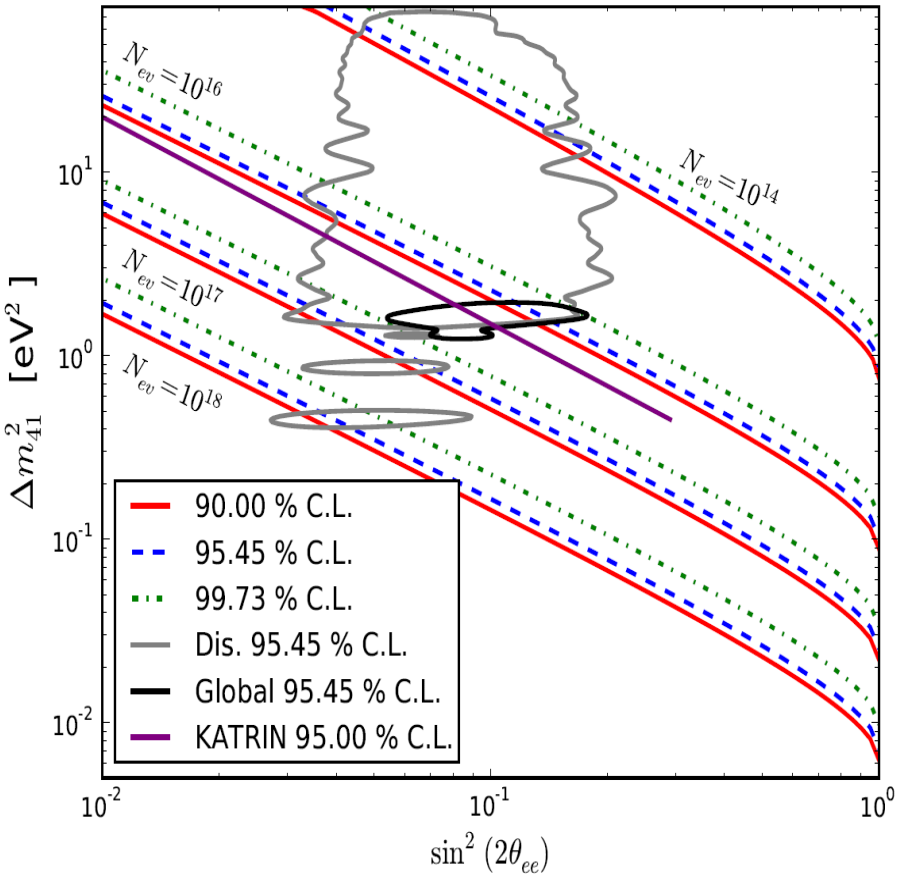

L. Gastaldo, C. Giunti, E. Zavanin., *High Energ. Phys.* **06** (2016) 61.

keV-scale sterile neutrinos

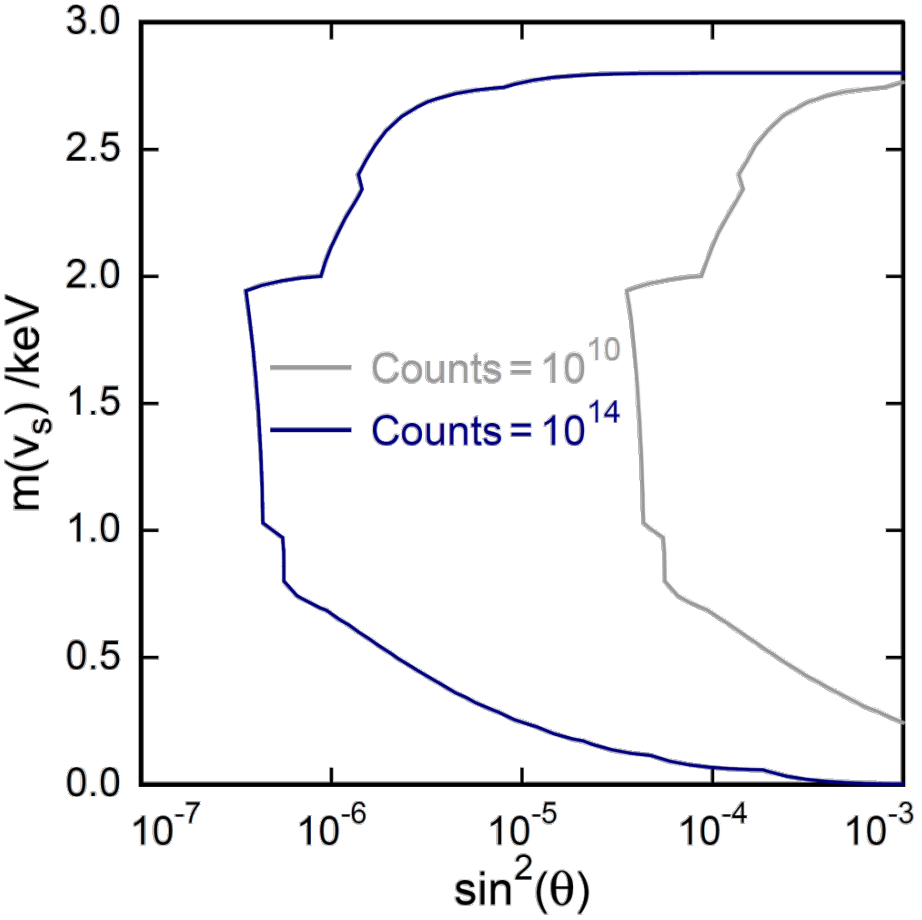

A White Paper on keV Sterile Neutrino Dark Matter, JCAP01(2017)025

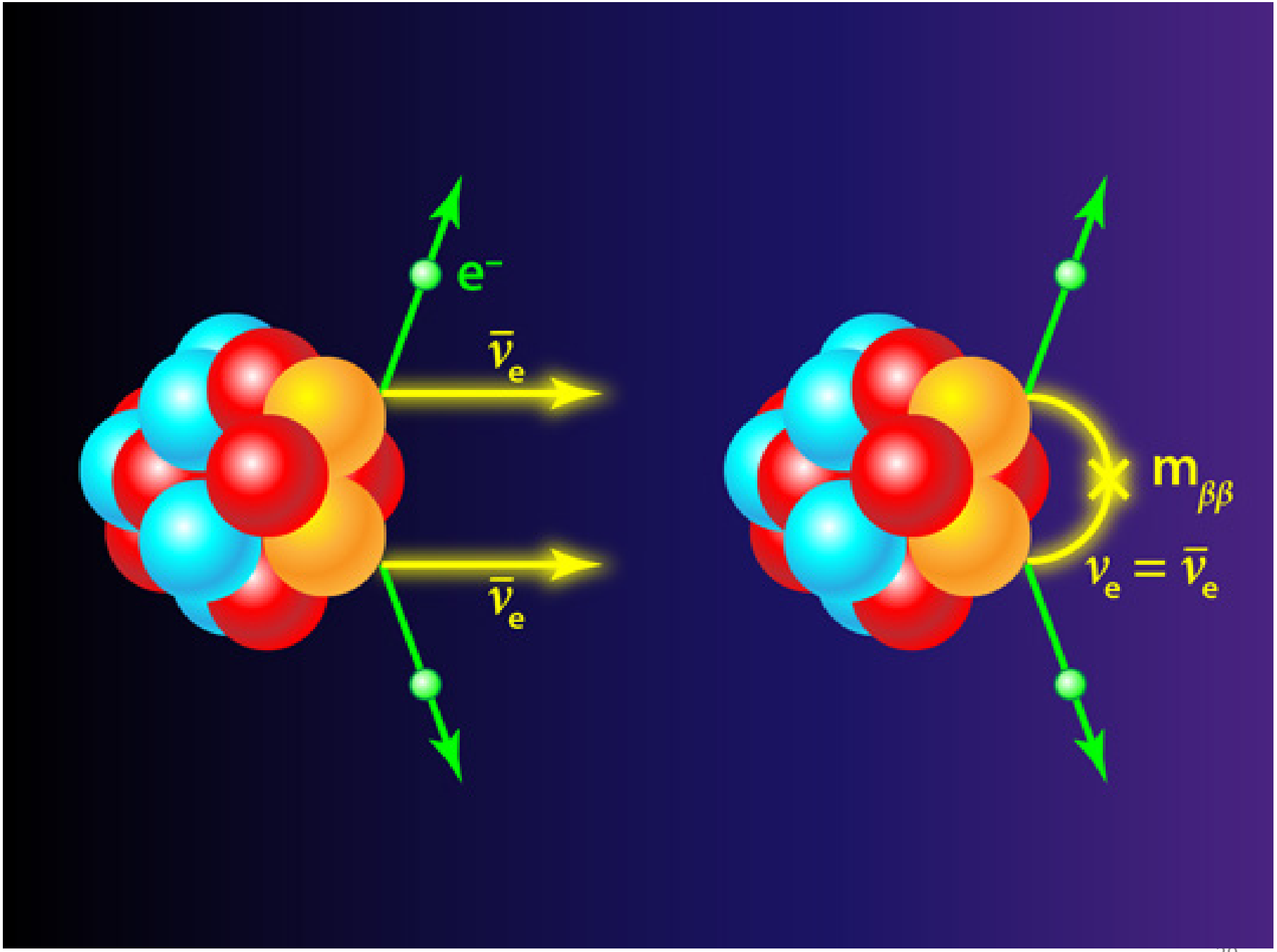

[Credit: APS/Alan Stonebraker]

Neutrinoless double beta decay

If conservation rules don´t allow simple beta decay:

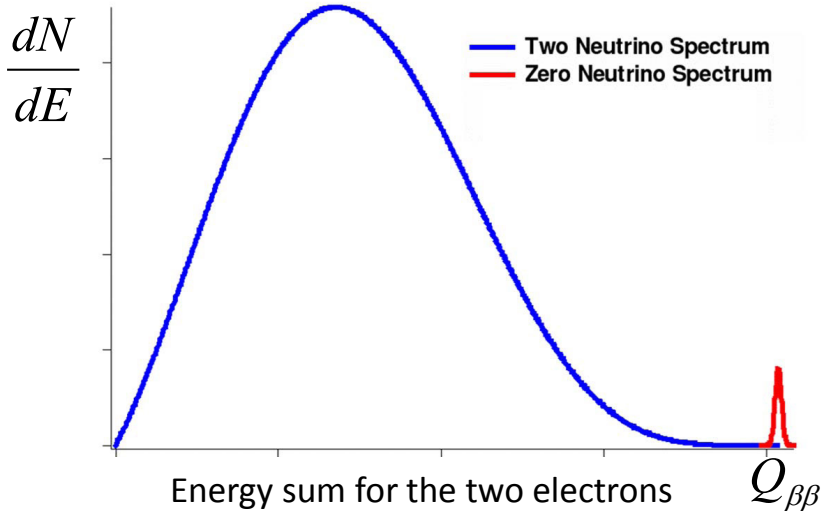

$2\nu\beta\beta$: (A,Z) → (A, Z+2) + $2e^-$ + $2\overline{\nu}_e$

$\tau_{1/2} \geq 10^{19}$ years

If $\nu = \overline{\nu}$:

$0\nu\beta\beta$: (A,Z) → (A, Z+2) + $2e^-$

$\tau_{1/2} > 10^{25}$ years

Measured for several nuclides

Never observed

Very rare events!

Promising technologies - Scintillating crystals

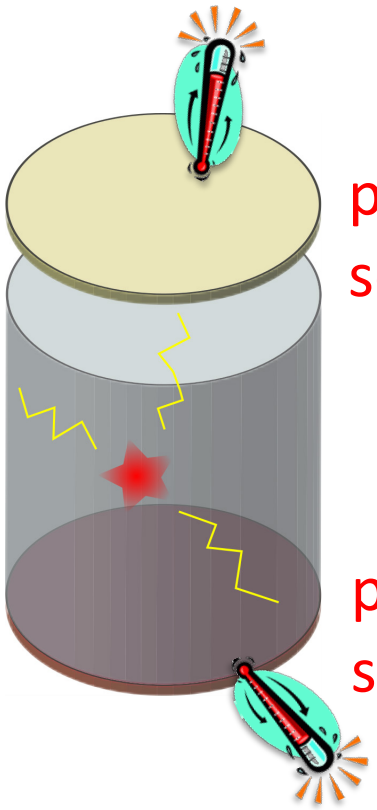

photon sensor

phonon sensor

Temperature signal: $\Delta T \cong \frac{\Delta E_{phonon}}{C}$

Light signal is also detected as $\Delta T \cong \frac{\Delta E_{photon}}{C}$ of a suitable photon detector

Promising technologies - Scintillating crystals

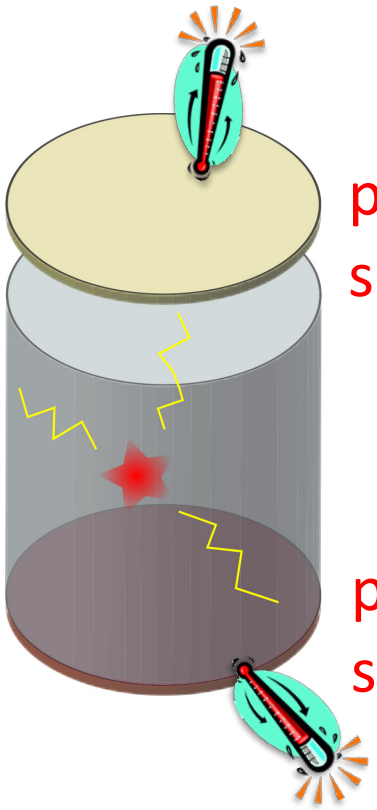

photon sensor

phonon sensor

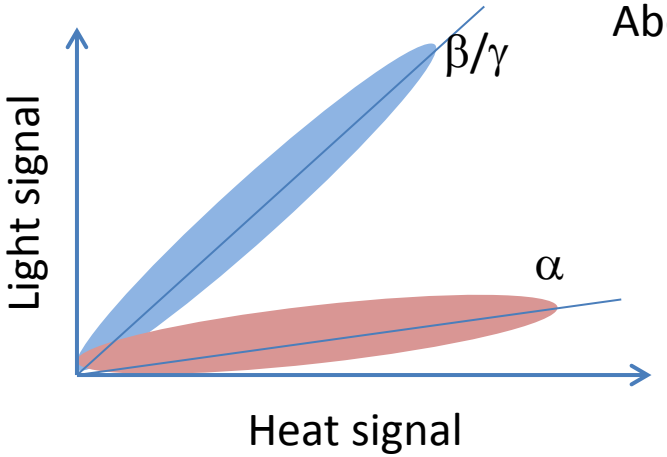

Promising technologies - Scintillating crystals

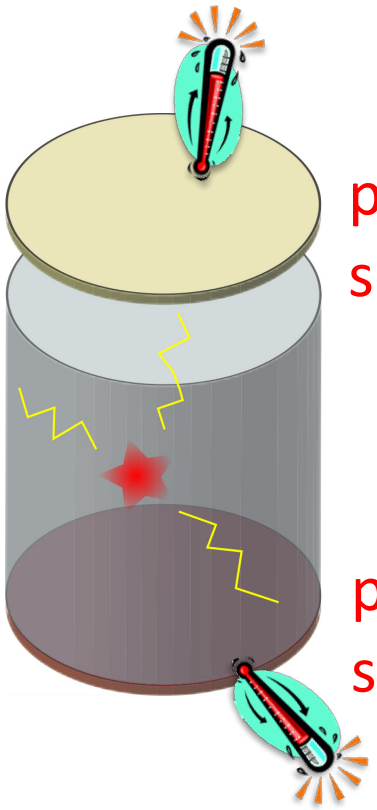

photon sensor

phonon sensor

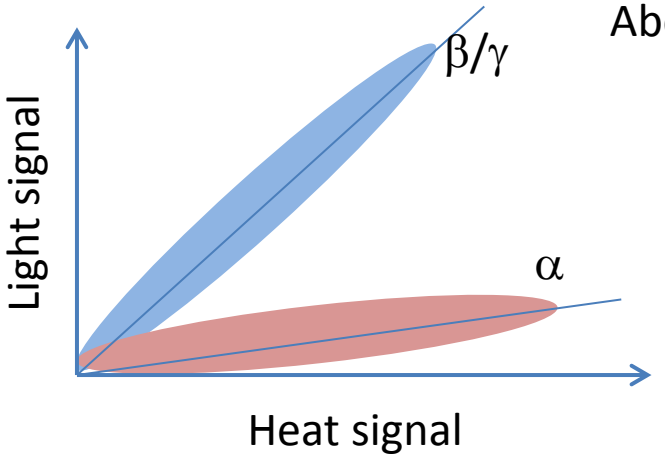

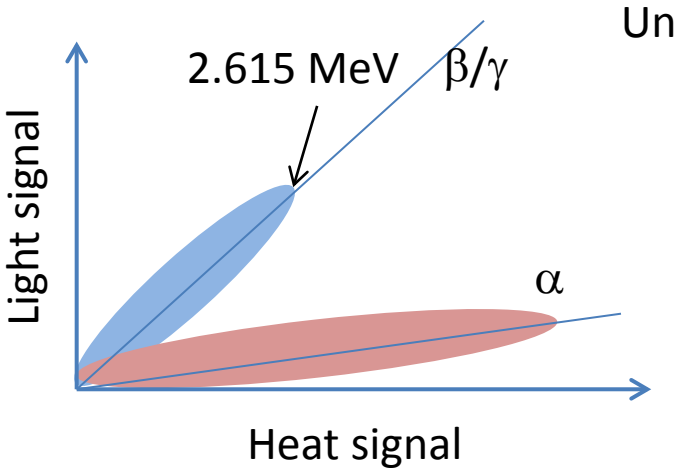

Background due to α particle can be removed

Promising technologies - Scintillating crystals

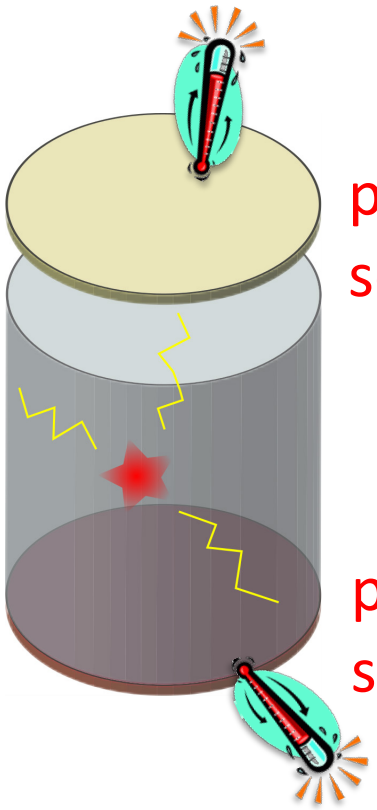

transition	$G^{01}(E_0, Z)$ $\times 10^{14} y$	$Q_{\beta\beta}$ [MeV]	Abund. (%)
$^{150}Nd \rightarrow {}^{150}Sm$ ←	26.9	3.667	6
$^{48}Ca \rightarrow {}^{48}Ti$ ←	8.04	4.271	0.2
$^{96}Zr \rightarrow {}^{96}Mo$ ←	7.37	3.350	3
$^{116}Cd \rightarrow {}^{116}Sn$ ←	6.24	2.802	7
$^{136}Xe \rightarrow {}^{136}Ba$	5.92	2.479	9
$^{100}Mo \rightarrow {}^{100}Ru$ ←	5.74	3.034	10
$^{130}Te \rightarrow {}^{130}Xe$	5.55	2.533	34
$^{82}Se \rightarrow {}^{82}Kr$ ←	3.53	2.995	9
$^{76}Ge \rightarrow {}^{76}Se$	0.79	2.040	8

Promising technologies - Scintillating crystals

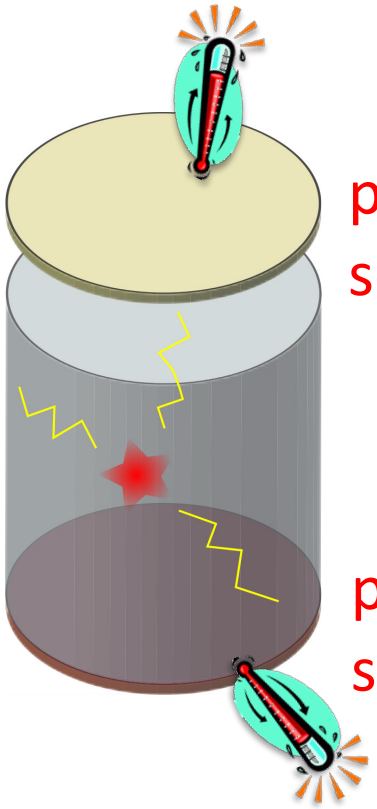

transition	$G^{01}(E_0, Z)$ $\times 10^{14} y$	$Q_{\beta\beta}$ [MeV]	Abund. (%)
$^{150}Nd \rightarrow {}^{150}Sm$ ←	26.9	3.667	6
$^{48}Ca \rightarrow {}^{48}Ti$ ←	8.04	4.271	0.2
$^{96}Zr \rightarrow {}^{96}Mo$ ←	7.37	3.350	3
$^{116}Cd \rightarrow {}^{116}Sn$ ←	6.24	2.802	7
$^{136}Xe \rightarrow {}^{136}Ba$	5.92	2.479	9
$^{100}Mo \rightarrow {}^{100}Ru$ ←	5.74	3.034	10
$^{130}Te \rightarrow {}^{130}Xe$	5.55	2.533	34
$^{82}Se \rightarrow {}^{82}Kr$ ←	3.53	2.995	9
$^{76}Ge \rightarrow {}^{76}Se$	0.79	2.040	8

AMoRE experiment with Molybdate crystals read out by **MMCs**

Technical Design Report for the AMoRE 0*νββ* Decay Search Experiment
https://arxiv.org/abs/1512.05957

AMoRE experiment

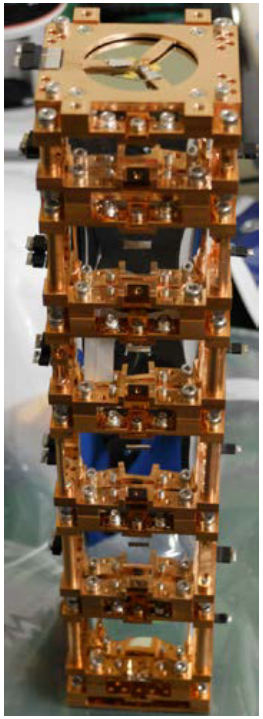

AMoRE-Pilot
1.9 kg
~ 2018

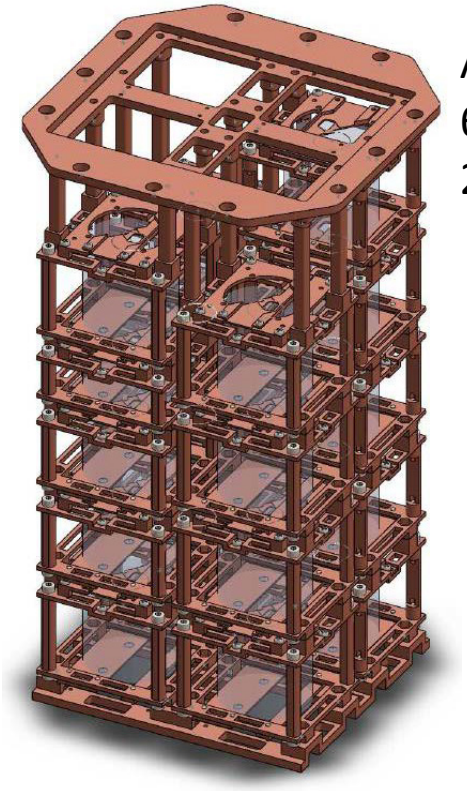

AMoRE-1
6kg
2019 ~

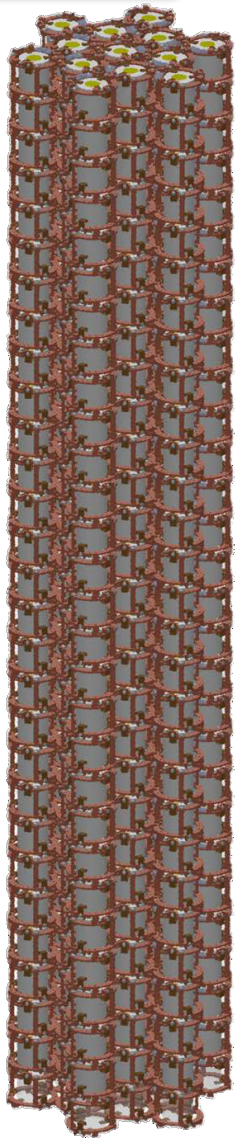

AMoRE-II
200 kg
2021 ~

AMoRE experiment

AMoRE-Pilot
1.9 kg

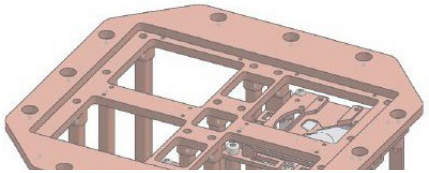

AMoRE-1
6kg

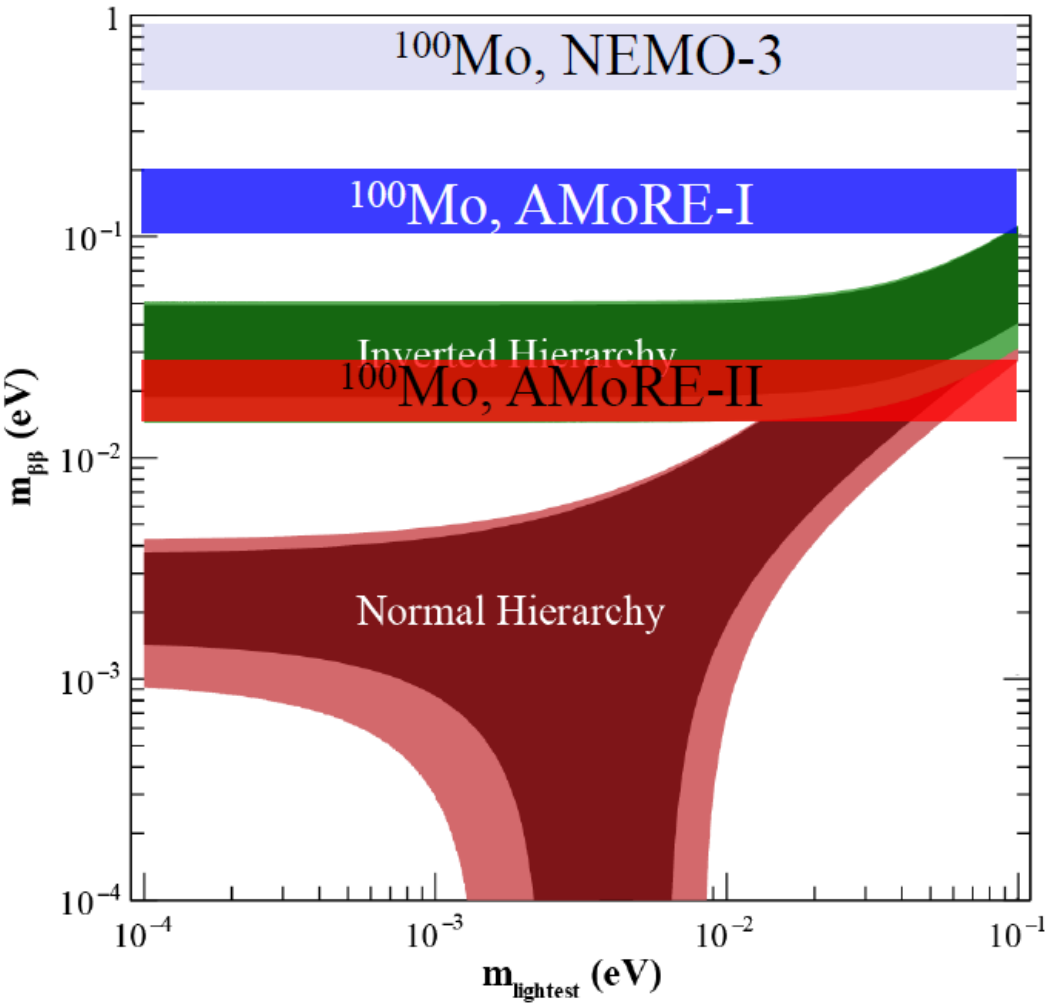

AMoRE-II
:00 kg
:021 ~

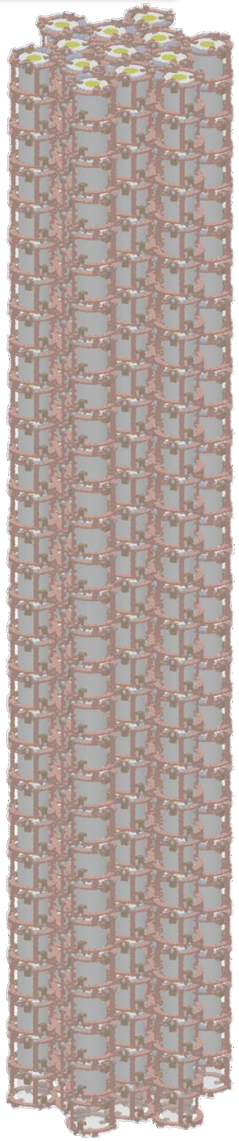

AMoRE detector modules

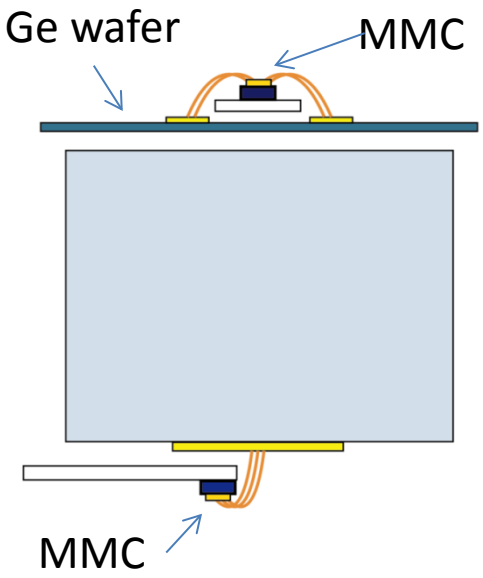

Light sensor at the top

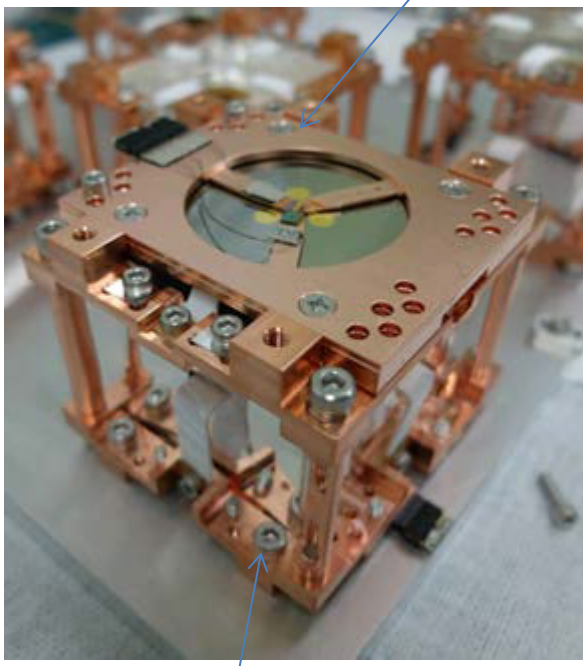

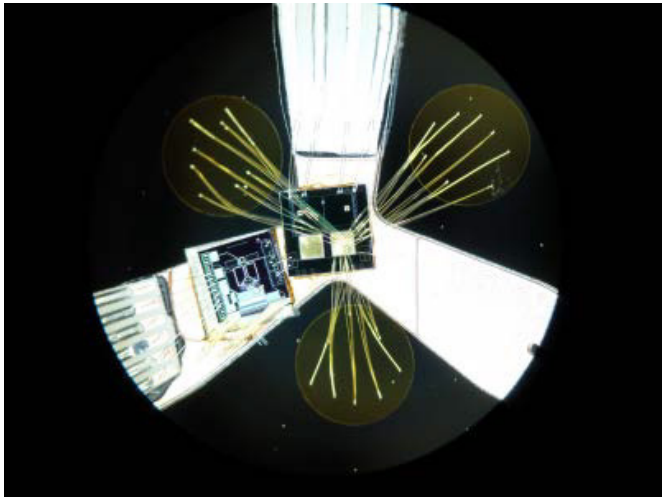

Phonon sensor at the bottom

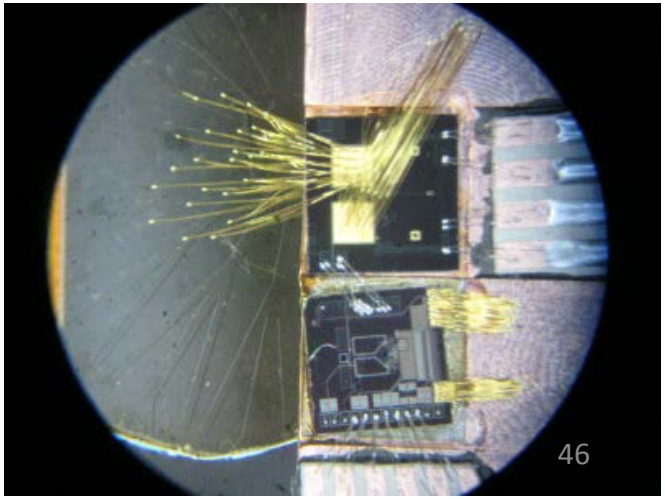

AMoRE detector modules

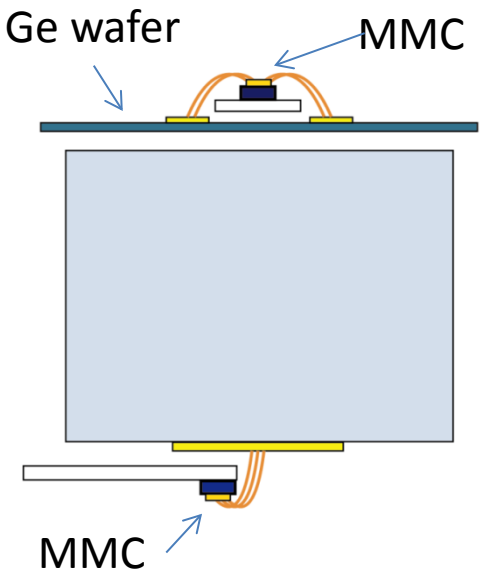

Light sensor at the top

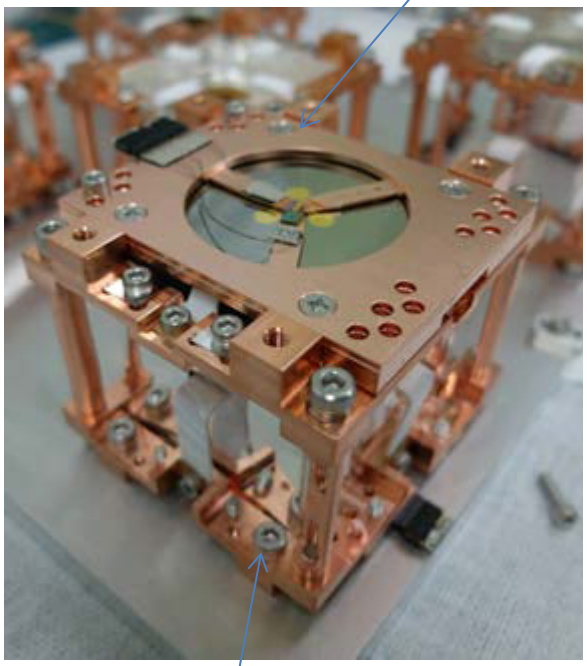

Phonon sensor at the bottom

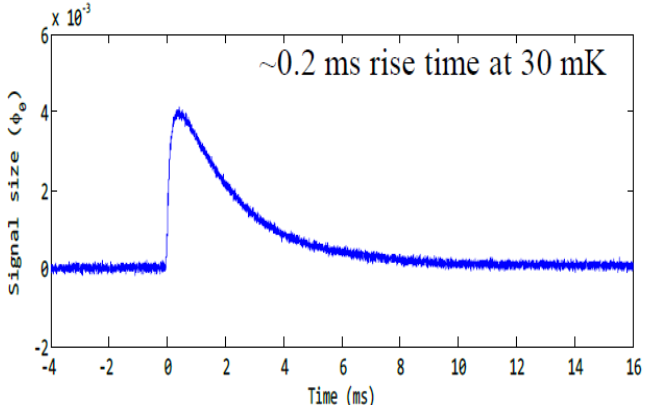

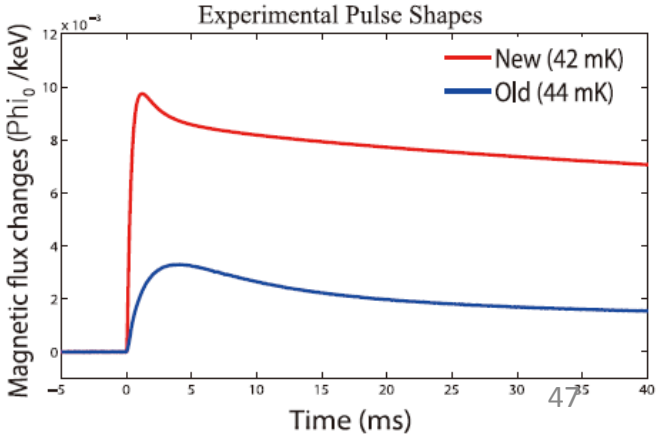

AMoRE detector performance

Particle discrimination by light heat ratio

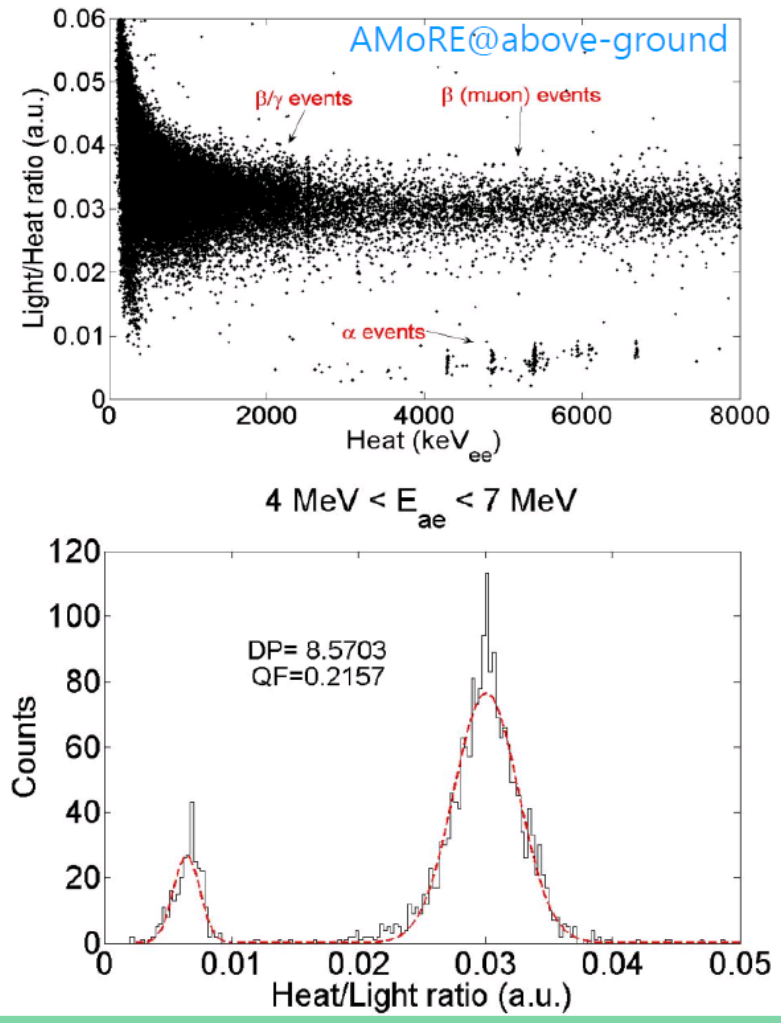

Phonon pulse shape discrimination (PSD)

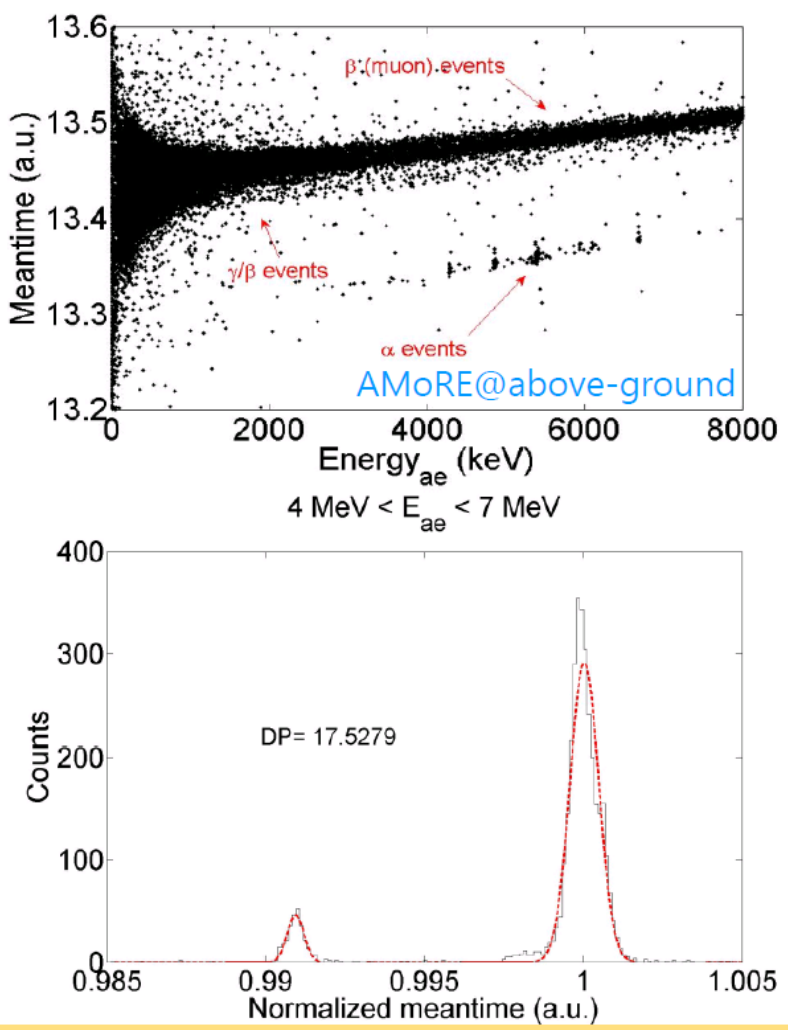

Alternative for AMoRE experiment

Combined Photon and Phonon Detector: P2

- Phonon detector:
  - energy resolution $\Delta E_{FWHM} < 100$ eV
  - rise time $\tau < 200$ µs
- Photon detector:
  - energy resolution $\Delta E_{FWHM} < 10$ eV
  - rise time $\tau < 50$ µs

Substrate: Ge or Si 3‘‘ wafer

- A minimum of (contaminated?) parts
- Position sensitivity possible

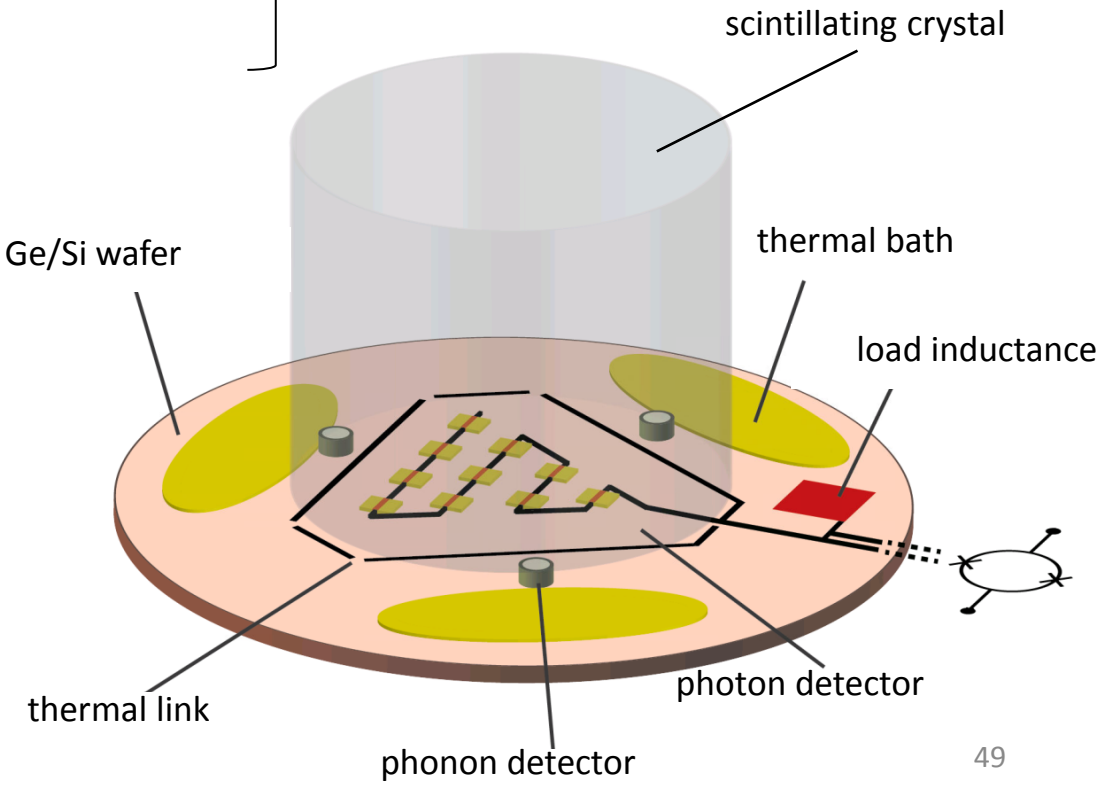

Integrated light and heat detectors P2

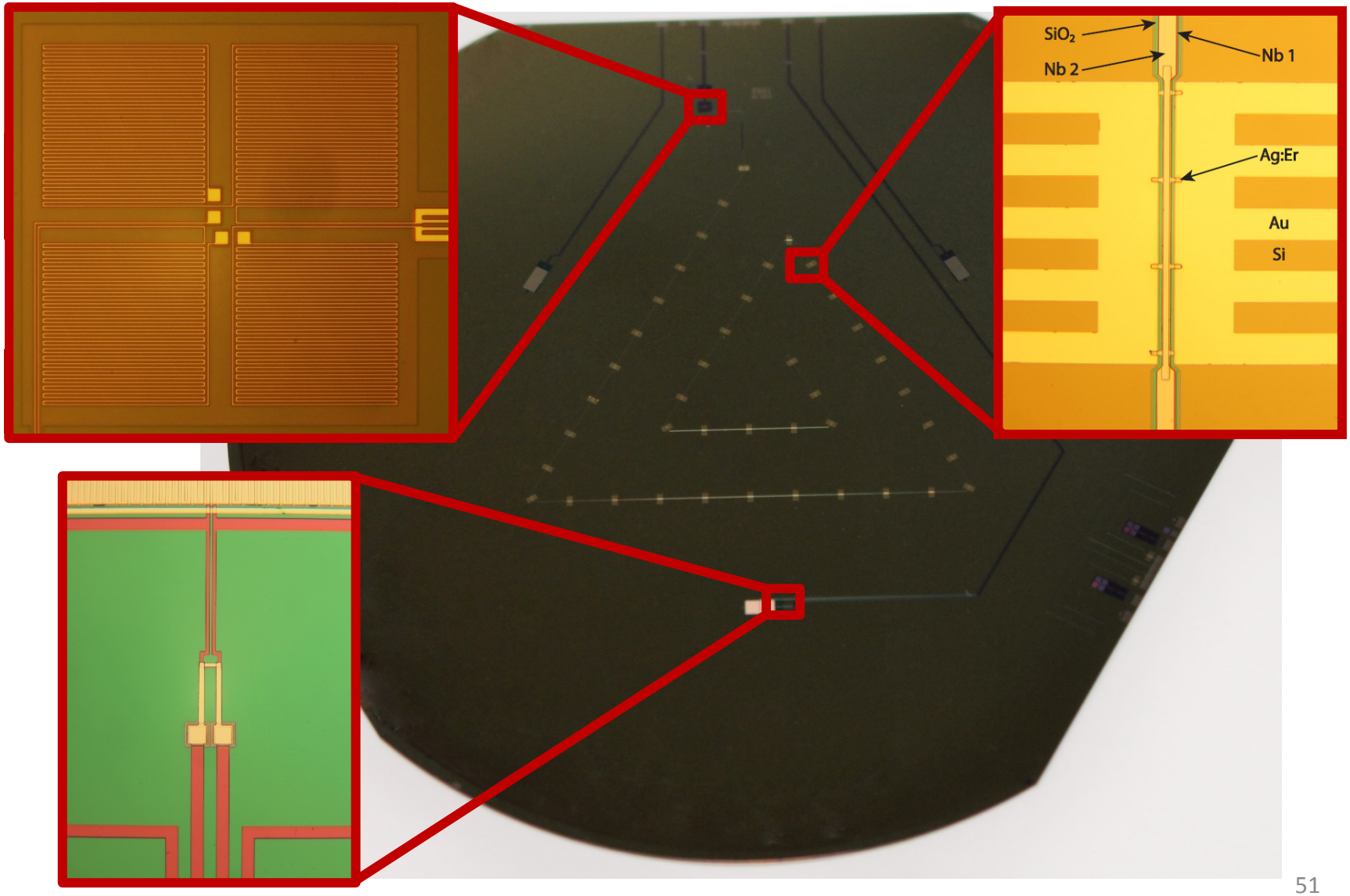

Integrated light and heat detectors P2

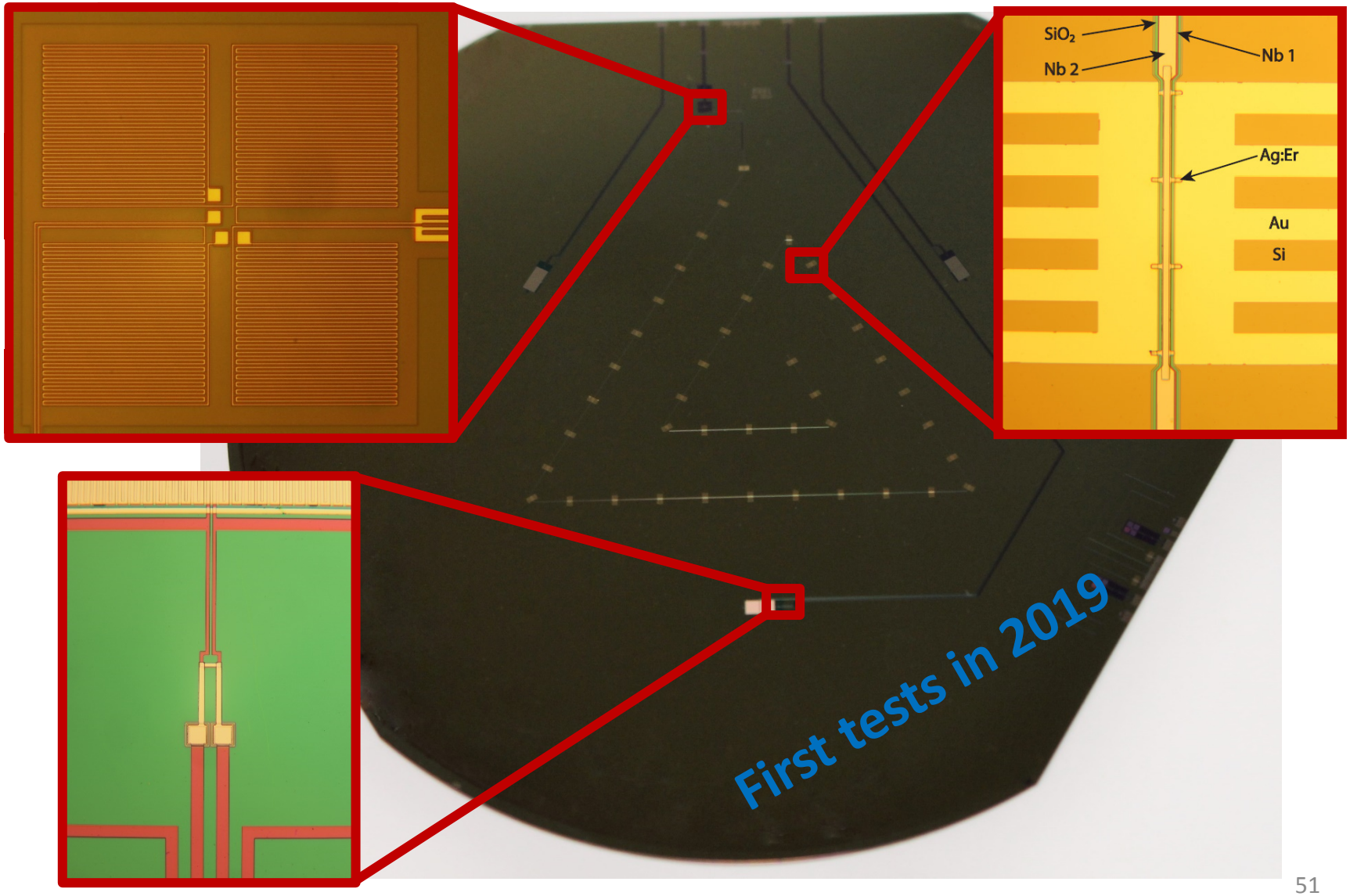

Conclusions

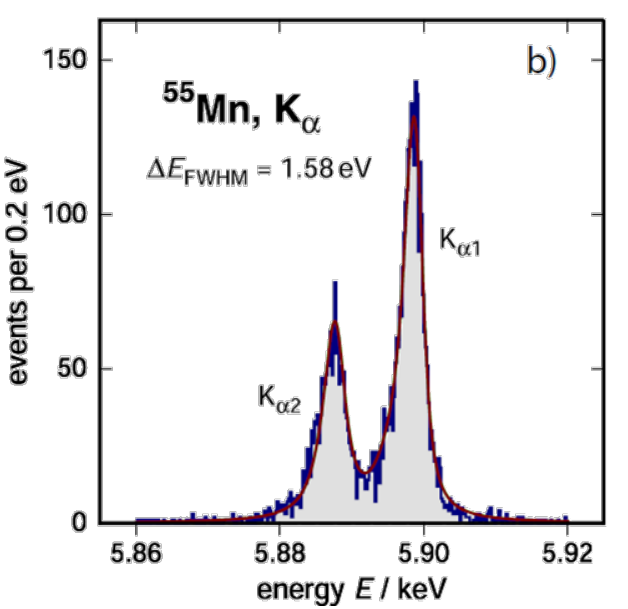

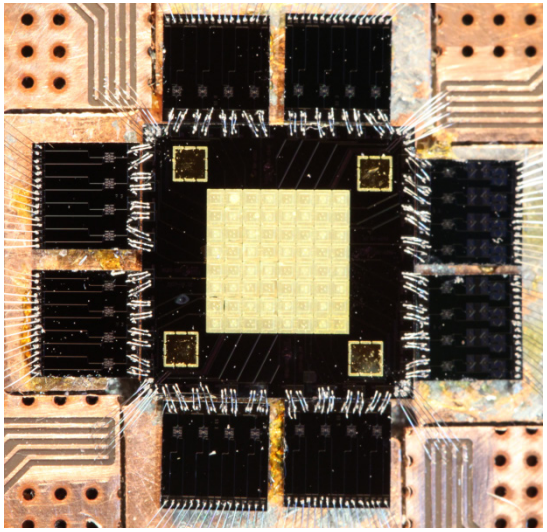

metallic magnetic calorimeters

- are versatile low temperature detectors
- high resolution for all kinds of particles
- wide range of energies

micro-farbrication works

- first detector arrays fabricated
- designed performance is reached

.....

Conclusions

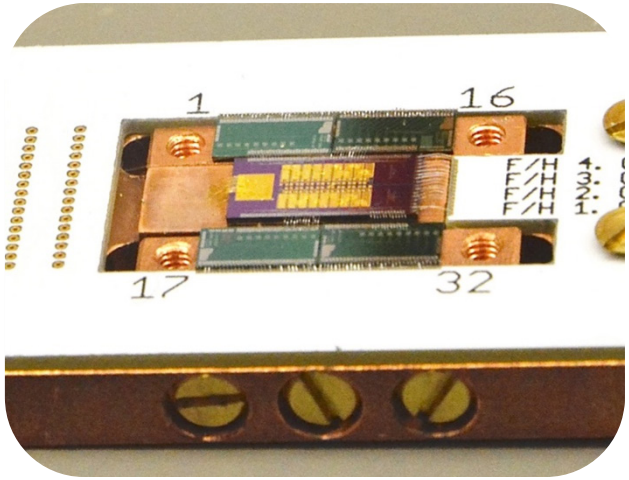

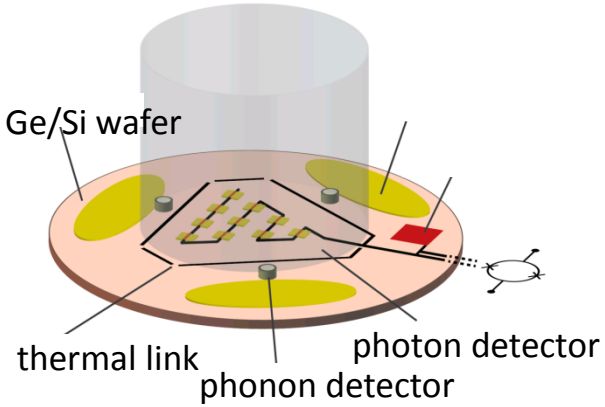

metallic magnetic calorimeters

- are versatile low temperature detectors
- high resolution for all kinds of particles
- wide range of energies

micro-farbrication works

- first detector arrays fabricated
- designed performance is reached

Perfect performance in ECHo

- Reliable implantation of ^{163}Ho

High potential for 0ν2β searches

- AMoRE experiment

Thank you!